THERMO-ECONOMIC ANALYSIS OF ORGANIC RANKINE POWER CYCLES USING PARABOLIC TROUGH SOLAR TECHNOLOGY

by

Mohammed Fouad Azfar Khan

A Thesis Presented to the Faculty of the
American University of Sharjah
College of Engineering
In Partial Fulfillment
of the Requirements
for the Degree of

Master of Science in
Mechanical Engineering

Sharjah, United Arab Emirates

December 2018

Approval Signatures

We, the undersigned, approve the Master's Thesis of Mohammed Fouad Azfar Khan.

Thesis Title: Thermo-Economic Analysis of Organic Rankine Power Cycles Using Parabolic Trough Solar Technology

Signature	**Date of Signature** (dd/mm/yyyy)
_____	_____
Dr. Mohamed Gadalla Professor, Department of Mechanical Engineering Thesis Advisor	
_____	_____
Dr. Zarook Shareefdeen Professor, Department of Chemical Engineering Thesis Committee Member	
_____	_____
Dr. Mohammad Nazzal Associate Professor, Department of Mechanical Engineering Thesis Committee Member	
_____	_____
Dr. Mamoun Abdel-Hafez Head, Department of Mechanical Engineering	
_____	_____
Dr. Ghaleb A. Husseini Associate Dean for Graduate Affairs and Research College of Engineering	
_____	_____
Dr. Richard T. Schoephoerster Dean, College of Engineering	
_____	_____
Dr. Mohamed El-Tarhuni Vice Provost for Graduate Studies	

Acknowledgments

I wish to thank my advisor, Professor Mohamed Gadalla, who has supported me throughout the thesis development and writing process. His guidance, academic knowledge and patience were crucial in completing this thesis.

Secondly, I would like to thank my committee members, Professor Zarook Shareefdeen, Professor Mohammad Nazzal, and the late Dr. Saad Ahmed for their time, feedback, and insightful comments. I wished to thank Dr. Mamoun Abdel-Hafez for guiding and supporting me through the Undergraduate and Master's Program at the American University of Sharjah. Also Thanking Dr. Ghaleb A. Husseini for his encouragement and support throughout my perusal for the Master's degree. I wish to thank the Graduate office members and registrar's office for their ongoing help and guidance throughout the graduate program.

Lastly, I would like to express my gratitude to the American University of Sharjah, for providing me with a graduate assistantship and the facilities and resources to carry out the research.

Dedication

To my parents, whose sacrifice and support has brought me to where I am in my life today. No amount of thanking would compensate for their care and unconditional love. To my sisters who provided me with their endless encouragement and support. To my friends, especially Adnan, who always helped and motivated me throughout writing my thesis.

Abstract

Diversifying into several renewable energy resources has become the goal for many countries striving for a sustainable future. Solar energy is currently one of the most reliable and abundant renewable resource that can be harnessed especially in the United Arab Emirates (UAE). Concentrated Solar Power (CSP) is currently the foremost solar technology able to convert solar radiation to useful heat energy. An Organic Rankine Cycle (ORC) is a variation to the Conventional Rankine Cycle (CRC), where the working fluid used is an organic fluid, which gives several advantages to the ORC such as a low turbine inlet temperature and the absence of moisture content in inlet fluid flow to the turbine, thus increasing plant life. A Regenerative Organic Rankine Cycle (RORC) is proposed to further improve the overall efficiency of the power block. The Parabolic Trough Solar Collector (PTSC) is one of the techniques used in collecting solar energy by concentrating the heat via highly deflective material to a pipe containing a heat transfer fluid (HTF). Thermal Energy Storage (TES) systems are integrated to store thermal energy, which can then be released when required based on the energy demand. Although TES increases the capital cost, it allows CSP to run during night hours to increase the solar share. This in turn improves the feasibility of the integrated system and further reduces carbon emissions. The Integrated Solar Organic Regenerative Rankine Cycle (ISORRC) with thermal energy storage is analyzed using thermodynamic and economic models. In this thesis, a 1 MWe output from the ORC is powered solely by solar energy from the PTSC, and the integrated system is then analyzed for TES with 0, 5 and 8 hours of operation to meet energy demands in rural areas and communities. The optimum fluid for the ORC cycle was found to be cyclopentane based on thermal efficiency and exergetic efficiency analyses. Hitec salt was found to be the optimum molten salt to be used for the TES system. Therminol VP-1 was found to be the optimum heating fluid for the PTSC system. It was concluded that the ISORRC, with 8 operating hours of TES, provides the best thermo-economic system to be implemented in UAE, providing a Levelized Cost of Electricity (LCOE) of 3.59 ¢/kWh and producing annual energy of 4,183,339 kWh.

Search terms: ***Concentrated solar power, parabolic trough solar collector, thermal energy storage, molten salts, regenerative organic Rankine cycles, organic Rankine cycles.***

Table of Contents

List of Figures

List of Tables

Nomenclature

A_a	Reflective aperture area	m^2
A_c	Glass cover area	m^2
A_r	Receiver area	m^2
C_p	Specific Heat Capacity of fluid	kJ/kg.k
$c_{p(HTF)}$	Specific heat capacity of Heat Transfer Fluid	kJ/kg.k
D_{co}	Glass cover outer diameter	mm
D_{ri}	Absorber tube inner diameter	mm
D_{ro}	Absorber tube outer diameter	mm
f	Fanning friction factor	-
F'	PTSC collector efficiency factor	-
f_D	Darcy friction factor	-
F_R	Heat removal factor	-
h	Enthalpy	kJ/kg
h_{cca}	Convective heat transfer coefficient between glass cover and ambient	$W/m^2.K$
h_{crin}	Convective heat transfer coefficient inside the absorber tube	$W/m^2.K$
h_{rca}	Radiation heat transfer coefficient between glass cover and ambient	$W/m^2.K$
h_{rcr}	Radiation heat transfer coefficient between glass cover and receiver	$W/m^2.K$
I_B	Normal beam radiation	W/m^2
k_f	Thermal conductivity of fluid	$W/m.K$
k_r	Thermal conductivity of the receiver	$W/m.K$
k_s	Thermal conductivity of the glass cover	$W/m.K$

L	Length of collector assembly	m
$\dot{m}_{HTF}$	Mass flow rate of Heat Transfer Fluid	kg/s
$\dot{m}_{air}$	Mass flow rate of air in Organic Rankine Cycle condenser	kg/s
$\dot{m}_{orc}$	Mass flow rate of fluid in Organic Rankine Cycle	kg/s
$\dot{m}_{salt}$	Mass flow rate of TES material	kg/s
N_c	Number of collectors	-
N_l	Number of loops	-
N_m	Number of modules	-
Nu	Nusselt Number	-
Nu_f	Nusselt Number of HTF	-
$Nu_{f_{laminar}}$	Nusselt Number of fluid for laminar flow	-
P	Pressure	kPa
P_c	Critical Pressure for ORC fluid	kPa
Pr	Prandtl Number	-
Pr_f	Prandtl Number of HTF	-
$\dot{Q}_{cond}$	Energy transfer in the condenser	kW
$q_{c,RORC}$	Specific heat rejected by regenerative organic Rankine cycle	kW/kg
$\dot{Q}_u$	Useful power collected by the PTSC	kW
Re_f	Reynolds Number of HTF	-
$\dot{S}_{gen}$	Entropy generated rate in the PTSC	kW/kg
T_{amb}	Ambient temperature	℃
T_c	Critical Temperature for ORC fluid	℃
T_{gc}	Glass cover temperature	℃
T_i	Inlet temperature for PTSC	℃
T_o	Outlet temperature from PTSC	℃

T_r	Receiver temperature	℃
T_s	Sun temperature	K
U_L	Overall heat loss coefficient	$\mathrm{W/m^2.K}$
U_o	Overall heat transfer coefficient	$\mathrm{W/m^2.K}$
v	Specific volume	$\mathrm{m^3/kg}$
v_f	Kinematic viscosity of fluid	$\mathrm{mm^2/s}$
V	Fluid velocity	$\mathrm{m/s}$
w	Collector width	m
w_{pump}	Specific pump work	kW/kg
$\dot{W}_{net}$	Net power output	MW
$\dot{W}_{net,RRC}$	Net power output in Regenerator Organic Rankine Cycle	MW
$\dot{W}_{turbine}$	Power output from Turbine	kW
$\dot{X}_{des,PTSC}$	Exergy destruction rate in the PTSC	kW
$\dot{X}_{in,PTSC}$	Exergy input rate to the PTSC	kW
$\dot{X}_{out,PTSC}$	Exergy output rate from the PTSC	kW
y	Flash factor	-

Abbreviations

CSP	Concentrated Solar Power
DHI	Diffused Horizontal Irradiance
DNI	Direct Normal Irradiance
EES	Engineering Equation Solver
HTF	Heat Transfer Fluid in the parabolic trough solar collector
ISORC	Integrated Solar Organic Rankine cycle
ISORRC	Integrated Solar Organic Regenerative Rankine Cycle
kWe	Kilowatt Electricity
kWhe	Kilowatt Hour Electricity
kWt	Kilowatt Thermal
kWht	Kilowatt Hour Thermal
LEC	Levelized Cost of Electricity
MENA	Middle East and North Africa
MWe	Megawatt Electricity
MWhe	Megawatt Hour Electricity
MWt	Megawatt Thermal
MWht	Megawatt Hour Thermal
NPV	Net Present Value
NS	Net Saving
ORC	Organic Rankine Cycle
PTSC	Parabolic Trough Solar Collector
RORC	Regenerative Organic Rankine Cycle
SAM	System Advisory Model
SRC	Simple Rankine Cycle
TES	Thermal Energy Storage

Chapter 1. Introduction

With the growing usage of fossil fuels and electricity worldwide, there is a growing interest in searching for renewable sources of energy to replace conventional methods of power generation. Solar Energy is a popular renewable source that can provide sustainable and clean source of power. Concentrated Solar Power (CSP) is one of the modern and efficient methods of extracting solar radiation that can be used for energy production. Parabolic Trough Solar Collectors (PTSC) systems are the most popular type of CSP that is used in the market for power generation. Organic Rankine Cycles (ORC) is an alternative method to conventional Rankine Cycle, where water is the working fluid used, whereas organic fluid is the working fluid that is used in the ORC. Recent studies have tackled how the use ORC as bottoming or supporting cycles to the simple Rankine Cycle improves the overall cycle efficiency. This thesis proposes the use of a direct Organic Rankine cycle as the main power generation cycle and studies its feasibility and operation.

1.1 Problem Statement

Currently, the world's oil producing countries are looking into diversifying their power generation. The United Arab Emirates has a vision for sustainability development and a significant involvement in the renewable energy sector. Renewable energy is a diverse sector including solar energy, biomass energy, geothermal energy and many more. Solar energy in particular is a topic of interest for power generation. Energy is extracted from solar radiation, using Parabolic Trough Solar Collectors (PTSC) which is fused to a Concentrated Solar Power (CSP) system. PTSC have a relatively lower cost as compared to other solar collectors, but their storage capacity is lower and is also dependent on the heat transfer fluid (HTF) used for the application. Thermal Energy Storage (TES) is a storage technique where energy from the solar collector is transferred to a two tank molten salts of Sodium Nitrate and Potassium Nitrate storage which can provide energy during night hours, and hence offer uninterrupted energy for even 24 hour operation periods. Organic Rankine Cycles are similar to Rankine Cycles except that the working fluid used is organic fluid. Organic Rankine Cycles are relatively new concepts where minimum usage of water is required and are able to generate electricity at a medium-low scale level.

1.2 Thesis Contribution

From the current sources of renewable energy sources, solar energy stands as the cleanest and the most secure and reliable of all. Using solar energy, as opposed to fossil fuels, reduces carbon dioxide emissions and has direct environmental benefits. Hence it is important to conduct research and invest within the renewable sector, specifically solar energy. Current Rankine Cycles (SRC) are most common within CSP systems. These systems require large amounts of water usage, which is also a key resource that is being worked on saving. Organic Rankine Cycles (ORC) help fill this void by using alternative working fluid to generate electricity. The ORC has great potential to meet residential demand on heat and power. It also has advantages over photovoltaic technology in terms of heat storage and ease in collecting energy; it also capable of supplying energy near point of usage [1]. Thermal Energy Storage (TES) allows storage of energy which can be used during night hours. This technology is crucial for the feasibility of CSP as power requirement is further accomplished. TES allows further extraction and usage of solar energy. Although capital costs increase, benefits include further reduction of carbon dioxide emissions and longevity of solar energy usage. Research in efficiently storing solar energy is being investigated as it goes hand in hand in reducing dependence on fossil fuels.

1.3 Scope and Objectives

The scope of this research is to study the usage organic fluids for power generation cycles and the utilization of renewable energy from the sun (solar energy) to power the cycle. After providing optimized solution of the Organic Rankine Cycle integrated with Parabolic Trough Solar Collectors and Thermal Energy Storage system, further evaluation on the operating cost of the system and the performance of the combined system is needed.

The main objective of this research is to provide an optimum organic fluid for the operation of the organic Rankine cycle, the selection of appropriate heat transfer fluid in the PTSC system and the sizing of the PTSC system to provide optimized integrated solution. TES system is used to increase the hours of operation of the system.

The research specifically aims to:

1. Conduct literature survey on the PTSC, ORC, TES and the integration of the systems.
2. Based on parametric analysis, conclude the optimum ORC working fluid and PTSC heat transfer fluid. TES capacity and optimal fluid is selected. Design points to be set at United Arab Emirates weather conditions to provide realistic results.
3. Carry out Energy and Exergy analysis on the Organic Rankine Cycle for optimum selection of working fluids.
4. Study the effect of modifying the Organic Rankine Cycle to a Regenerative Organic Rankine Cycle by adding components to improve cycle performance.
5. Conduct Parametric analysis to obtain the convective heat transfer coefficient inside the absorber tube of the PTSC, selection of the solar collector and receiver.
6. The daily, monthly and annual operation characteristics of the integrated system is studied.
7. Analyze the levelized cost of electricity and capital cost of the system.

1.4 Research Methods and Materials

Literature review and research material are compiled for the American University of Sharjah library research database from journal article and published research papers. The selection of organic fluid of the Organic Rankine Cycle is targeted first. Chemical Properties of Organic Fluids are taken from EES library (Engineering Equation Solver Library). These fluids are grouped based on their critical temperature and critical pressure and energy, and exergetic analysis is done to select the best ORC fluid. Heat Transfer fluid to be used in the Parabolic trough solar collector is researched and analyzed. Therminol VP-1, Therminol 66 and Syltherm are compared as the heating fluids in the PTSC. Based on parametric results for convective heat transfer coefficient of using these fluids based on their chemical and physical properties, the optimum heat transfer fluid for the application is selected using MATLAB software. Parametric analysis is done to study the performance of the design PTSC.

The Organic Rankine Cycle is designed on the Engineering Equation Solver (EES) as it has the thermophysical properties of refrigerants and various fluids data which can be used to design the ORC. Modifications to the Simple Organic Rankine

Cycle are also studied on EES and the effects of efficiency and performance are examined. The PTSC and TES system complete analysis is done on the System Advisory Model (SAM) software. Its inbuilt data for solar field's analysis and United Arab Emirates weather reports provide optimum tools for our application. Finally, the integrated system analysis is done where the PTSC powers the ORC with TES storage, and its results are discussed.

1.5 Thesis Organization

This thesis is organized as follows: Chapter 1 gives an introduction to the thesis, clarifies the significance of the research and provides the problem statement. It also states the scope and objectives of the thesis, and highlights the research methodology used in the analysis. Chapter 2 includes the literature review of the thesis. Research papers and journal articles are compiled on the Organic Rankine Cycle, Parabolic Trough solar collectors and Thermal Energy Storage systems. The chapter also sheds light on the organic fluids and heat transfer fluids that can be used for application. The system is designed, and modeling equations are set for the application in Chapter 3. The results and discussion of the results are presented in Chapter 4. Chapter 5 concludes the thesis with the conclusion and further recommendation and remarks.

Chapter 2. Background and Literature Review

This chapter includes a detailed literature survey about Organic Rankine cycles, solar energy and PTSC's and their applications.

2.1 Organic Rankine Cycles and Solar Energy Applications

GeoModel Solar [1] provides data for annual DNI ratings as well as the global horizontal irradiation (GHI) levels in the UAE as recent as 2013 and 2011 respectively. The readings show that the UAE is placed in a very favorable position to capture solar energy with high DNI and GHI readings. This potential has led to considerable research in the UAE for further implementation and usage of solar energy technologies. Figure 1 illustrates the average annual sum DNI for the UAE from the years 1999 till 2011. Figure 2 illustrates the average hourly solar insolation in Abu Dhabi based on the research.

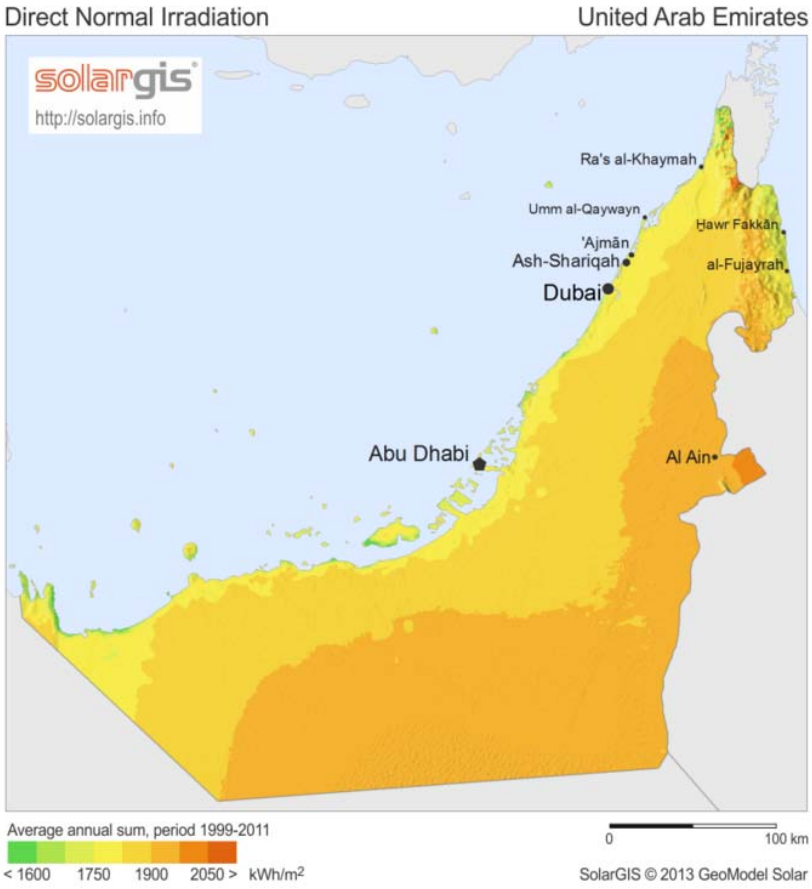

Figure 1: Average annual sum DNI for a period from 1999-2011 [1]

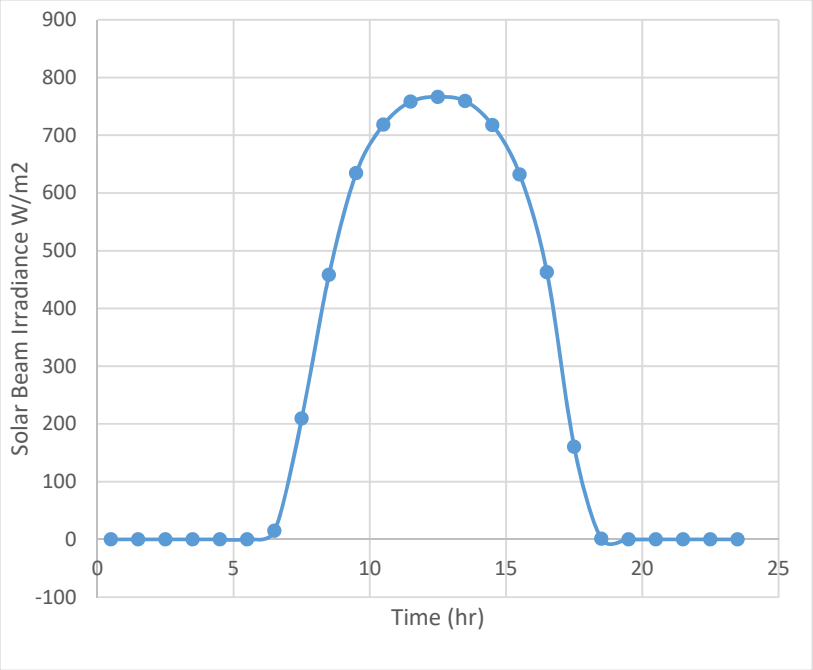

Figure 2: Annual average hourly solar radiation in Abu Dhabi [1]

Xu et al. [2] inspect the performance of a direct vapor generation (DVG) supercritical organic Rankine cycle (SORC) which is powered by linear Fresnel reflector (LFR) concentrator. The system was modeled through EES. They also propose a technique to select suitable supercritical organic working fluids for mid-high temperatures (150 °C–350 °C). Their results show that introducing both DVG and supercritical technologies decrease irreversibility of the evaporator, reduce the heat lost and improves overall efficiency of the system.

M. Marion, Voicu and Tiffonnet [3] present the potential of producing mechanical power by a system combining solar thermal collector with an organic Rankine cycle (ORC). A subcritical Rankine cycle was simulated for organic fluids R134a, R227ea and R365mfc operating between the solar collector and a fixed temperature sink. It was observed that the net mechanical power depended heavily upon the fluid mass flow rate.

Zhou [4] investigates the hybridization of solar and geothermal energy in a super critical organic Rankine cycle in order to identify the benefit generated from potential synergies of a hybrid system. The system was compared with subcritical

hybrid plant, standalone solar and geothermal plants. The results of the analysis show that the hybrid plant using supercritical organic Rankine cycle outperforms the hybrid plant using subcritical organic cycle by producing 4-17% more electricity from the same energy resources. From the economical point of view, a hybrid plant using supercritical organic Rankine cycle has solar-to-electricity cost of approximately 1.5-3.3% less than the subcritical scenario.

Quoilin, Broek, Declaye, Dewallef and Lemort [5] provide a clear comparison between the organic Rankine cycle and the steam Rankine cycle. One of the main differences between organic fluids and water is that the slope of the saturated vapor curve (right curve of the dome) is negative for water, while the curve is much closer to vertical for organic fluids. As a consequence, the limitation of the vapor quality at the end of the expansion process disappears in an ORC cycle, and there is no need to superheat the vapor before the turbine inlet. This results in lower turbine inlet temperature and increases the life of the turbine from 10-15 years to over 30 years. Common working organic working fluids that have been commercially applied are also shown in Table 1.

Table 1: Common ORC working fluids commercially installed [5]

HFC-134a	Used in geothermal power plants or in very low temperature waste heat recovery
HFC-245fa	Low temperature working fluid, mainly used in waste heat recovery.
n-pentane	Used in the only commercial solar ORC power plant in Nevada. Other applications include waste heat recovery and medium temperature geothermal.
Solkatherm	Waste heat recovery
Octamethyltrisiloxane (OMTS)	Biomass-CHP power plants
Toluene	Waste heat recovery

Feng, Zhang, Li, Yang and Shi [6] investigated the thermoeconomic comparison of Regenerative organic Rankine cycles and basic organic Rankine cycles. Five parameters were examined including pinch point temperature difference, condenser temperature, evaporator outlet temperature, degree of superheat, and degree of supercooling on the levelized energy constant exergy efficiency. The study also compared the multi-objective approach of maximizing energy efficiency and minimizing levelized energy cost with other available solutions. Research showed a negative correlation between economic factor sand thermodynamic performance. The ideal exergy efficiency and levelized energy cost for the Pareto-optimal solution of the regenerative organic Rankine cycles were 55.97% and 0.142 $/kWh, respectively, which were 8.1% greater exergy efficiency and 21.1% higher levelized energy cost than that of the basic organic Rankine cycles under the conditions being studied. The study found that highest exergy and thermal efficiencies appear alongside lowest net power output and worst economic performance.

Meroni, Andreasen, Persico and Haglind [7] presented an alternative approach to choosing the working fluid for multistage axial turbine containing organic Rankine cycle units. The method was tested on a marine diesel engine for recovery of waste heat. This approach allowed the researchers to select the best working fluid accommodating for the use of cycles using multistage turbine designs. It was found n-butane generated the best results in maximization of turbine and cycle in terms of efficiency, turbine cost and cycle net power output. The study demonstrated that the design application can vary from a lone turbine featuring supersonic converging-diverging nozzle, to a more prudent multi stage turbine with supersonic converging nozzles and post expansion.

Zhai, An and Shi [8] proposed a design method for selecting zeotropic mixture working fluids for organic Rankine cycle, as opposed to pure working fluids. The study suggests that zeotropic mixtures can achieve better results than conventional pure working fluids. The design aims to find zeotropic mixtures with essentially the same properties as the pure working fluids as well as temperature glide compatible with the cooling source, where temperature glide is the difference between the saturated liquid temperature and superheated vapor temperature for a fluid at a fixed pressure. The study evaluated the effect of the mixture's temperature glide on the cycle performance.

Katulić, Čehil and Schneider [9] studied the thermodynamic enhancement of a bottom cycle that utilizes organic fluids and water as working fluids. The heat recovery steam generator was designed with consideration of different pressure levels, the reheat of the first pressure level, the arrangement of the heat-exchangers network in which heat can be traded between working fluids and flue gas. The first pressure level used water while the second used organic fluid. The functioning outlines of the working fluid at each pressure level and reheat, and the different parameters of the heat exchangers inside the heat recovery steam generator (HRSG) were weighed while improving the thermodynamic efficiency of the bottom cycle. The study demonstrated that a better thermodynamic performance could be gained by implementing parallel and series configurations of water and heat exchangers in the first pressure level and organic working fluids in the second pressure level.

Györke, Deiters, Groniewsky, Lassu and Imre [10], presented a better way to categorize pure working fluids for organic Rankine cycle to aid in acquiring thermodynamically the best working fluid for a given source of heat. This is in contrast to the currently available classification which is simply divided into three broad categories of dry, wet and isentropic working fluids.

Lukawski, DiPippo and Tester [11] utilized the molecular composition of the working fluids being used to demonstrate a way to determine the efficiency of organic Rankine cycle plants. The study based its assessment on molecular group contribution. This was done by comparing the critical temperature and reduced ideal gas capacity of the working fluid with the peak utilization efficiency η_u of an organic Rankine cycle plant. The authors managed to calculate the utilization efficiency with an average error of 0.9-1.5 % points. They were also able to estimate the ideal organic Rankine cycle heat source temperature Ths with an average error of 3.5 °C to 6.6 °C. The method was implemented on 92 working fluids that have a limited association with global warming and that are less flammable.

Sanchez, Gosselin and Da Silva [12] examined the use of dual zeotropic mixtures as working fluids in organic Rankine cycles. the study aimed to find the optimal zeotropic mixture that would lessen the heat exchanger's global conductance at select temperatures of the heat source while attaining the highest total power and

exergetic efficiency. This was done by analyzing 28 possible dual mixtures by combining two hydrofluorocarbons and six hydrocarbons. These combinations were evaluated using a basic Rankine cycle keeping the heat source temperature as an independent property. The heat source temperature was set at six different values with increments of 20°C, from 80 °C to 180°C. The study found that the list of ideal zeotropic mixtures slims down as the heat source temperature rises.

Dong, Xu, Li, Quan and Wen [13], examined the cost effectiveness and the thermodynamic ability of the low grade organic Rankine cycles using zeotropic versus pure working fluid mixtures. The study also showed the impact of factors such as size of the heat exchanger, economical capability, heat source temperature and mixture mass friction on the total power output. The study demonstrated that zeotropic organic Rankine cycle produced greater total power than pure organic Rankine cycle, more so for a heat source with a bigger difference in temperature. However, cost-effectiveness is reduced due to the need for a greater heat exchanger area. The authors found that there is a need to determine whether the energy requirement can be met in pure organic Rankine cycle under the provided pinch point terms before the choice between zeotropic mixtures and pure working fluid can be made.

Bellos and Tzivanidis [14] designed a system that has the ability to maximize electricity output by the use of waste heat in a solar powered hybrid organic Rankine cycle. The parabolic trough collectors were linked to a storage tank, that supplied the heat recovery system, which used waste heat at low temperatures of 150°C-300°C. The study investigated four different working fluids, MDM, toluene, cyclohexane and n-pentane, in the modified organic Rankine cycle model. The study found that toluene showed the highest formation of electricity, followed by cyclohexane MDM and pentane. For the given temperature range of the waste heat, the electricity production with toluene was documented as being between 479kW and 845 kW and the model efficiency between 11.6% and 19.7%. The study also demonstrated that the higher the temperature of the waste heat source, the greater the amount of waste heat received by the organic Rankine cycle for all the working fluids tested.

Saloux, Sorin, Nesreddine and Teyssedou [15] proposed a remodeled approach of a conventional thermodynamic cycle that permits the computation of thermodynamic

factors such as pressures, mass flow rated and temperatures. The authors also presented a technique for choosing the fittest organic working fluid for any given design criteria. To highlight the promising application for the model being discussed, the entire process was demonstrated through a case study.

Yang Ding et al.[16] presented an exergoenvironmental design of the organic Rankine cycle. Working fluids R134a, R245fa and R227ea were used to demonstrate the environmental burden of working fluids in each section of the organic Rankine cycle system, based on the exergy loss of the matching part. The study showed that the tested environmental burden of the working fluids could not be overlooked. R134a had an impact of 13.76%, R152a 2.26%, R227ea 26.04% and R245fa had an impact of 14.77% on the whole setup. The environmental burden due to spillage of working fluid was 67.52%, 35.71%, 75.62% and 68.34% respectively. Therefore, the organic Rankine cycle with the least exergo-environmental impact was found to be the system that had used R245fa.

Yang, Cho, Zhang, Zhang and Wu [17] estimated optimization and performance of Organic Rankine Cycle, based on Artificial Neural Network (ANN), to recover heat wasted in diesel engines. The outcome of seven chief operating specifications on the energy output of the Organic Rankine Cycle system were examined, using an artificial neural network based prediction format that took into account the coefficient of correlation and the mean squared error. The study also investigated the usage of a genetic algorithm to increase precision of the estimates. The study found that using the genetic algorithm decreased prediction error when used along with the artificial neural network as compared to the use of the artificial neural network on its own. It showed that when compared to the experimental data, peak relative error was found to be less than 5%. It was suggested that further readjustment of more operating parameters could result in greater energy output while conducting the experiment.

Braimakis and Karellas [18] explored the outcome of exergetic optimization of double stage organc Rankine cycle on waste heat recovery. The goal of the study was to find out the ability to better the exergetic efficiency of double stage organic Rankine cycle in comparison to single stage cycles and to determine the parameters to gain maximum total power output for heat source temperatures between 100 ℃ to 300 ℃.

The study found that, contingent to the working fluids being used and temperature of the heat source, double stage organic Rankine cycles can achieve a relative rise in exergetic efficiency of up to 25%, as compared to single stage organic Rankine cycles. It also concluded that when the heat source temperature is below or between the critical temperatures of the organic fluids being used in their two stages, double stage organic Rankine cycles show an especially encouraging outcome.

Li, Ge, Luo and Tassou [19] explored low-grade energy generation models with R245fa organic Rankine cycles and CO_2 transcritical power cycles. The major constituents of each of the models tested included a turboexpander with high-speed generator, a liquid pump, a finned-tube air cooled condenser and a plate-type gas generator. Indirect heat from gases of an 80 kWe micro-turbine CHP unit was used to test the two models through a hot thermal oil system. The study examined the outcome of the performance of each model when certain dynamic processes were tested; this included system startup and shutdown, variation in the speed of the oil pump and the change in the speed of the working fluid pump. Results showed that the startup and shutdown processes and the pressure and temperature at the inlets and outlets of turbines, have a great impact on the mass flow rate of the working fluid.

White, Oyewunmi, Chatzopoulou. [20] put together a computer-aided molecular design of the organic Rankine cycle working fluid using the statistical associating fluid theory Mei equation of state, and thermodynamic augmentation, along with heat-exchanger sizing models, thermoeconomic analysis, and costing of parts. This method allows for quicker and more advanced calculation of potential thermodynamic augmentation of the organic Rankine cycle and working fluid, along with the ability to perform thermoeconomic analysis to create the most functionally and financially efficient model. The combination of computer-aided molecular design with organic Rankine cycle method helped compute the most suitable cycles and working fluids and their behavior when exposed to three different heat sources with temperatures set at 150 °C, 250 °C and 350 °C. The best combination of organic Rankine cycle model and working fluid was determined for each heat setting as well as the cost of each model. The study found that the most cost effective fluids were not necessarily the ones that had the greatest power output. Fluids with the least specific-investment costs were found to be isoheptane at £ 5620, 2-pentane at £ 2760 and 2-heptene at 2070 pound

sterling per kW. The corresponding power outputs were 32.9 kWt, 136.6 kWt and 213.9 kWt respectively.

Habibollahzade, Gholamian, Ahmadi and Behzadi [21] proposed an energy system that combines a Rankine cycle, a proton exchange membrane, a thermoelectric generator and a parabolic trough collector. The thermoelectric generator is to replace the condenser and so the extra power generated from the thermoelectric generator can be used by the proton exchange membrane electrolyzer to create hydrogen. The system performance was evaluated with the exergy and economic aspects in mind. Results showed that with a good balance between the ideal working conditions for maximum exergy and economic efficacy , exergy efficiency would be 13.29% at a cost of 63.96 $/GJ. They concluded that replacing the condenser with a thermoelectric generator would improve the system as well as reducing total cost.

Mahmoudi, Fazli and Morad [22] summarized the available practical and theoretical research on organic Rankine cycle technology in many different situations. The study aimed to audit available literature from the last four years with regards to the experimental use of organic Rankine cycles for utilizing wasted heat and the factors effecting its overall performance such as working fluids, conditions for operation and cycle configuration. The data collected was used to demonstrate the relationship between the type of heat source and the working fluid used in different conditions.

H. Nami, Nemati and Fard [23] conducted an exergy analysis on geothermal driven dual fluid organic Rankine cycle to examine how different parts of the model interact with each other. The system was put through various operating conditions so that real, unavoidable and ideal performances could be studied. The rate at which exergy was destroyed was split into exogenous, endogenous, unavoidable and avoidable parts to be able to get a closer look at the effects of components inefficiency on each other, exergy loss and the possibilities of improvement. The conventional examination revealed that the condenser, high pressure vapor generator and low pressure vapor generator are the most vital components by 15.93%, 29.98% and 38.11% of the overall rate at which exergy is being destroyed, respectively. The advanced analysis demonstrated that only 15% of the conduction exergy loss is avoidable, which includes 7% of avoidable exergy loss rate of the model. Low pressure vapor generator,

low pressure turbine and high pressure vapor generator were also found to be the most vital components when looking at advanced exergy because of their autogenous avoidable exergy loss rates.

Seyedkavoosi, Javan and Kota [24] conducted an exergy analysis for waste heat recovery from an internal combustion engine in a two-parallel-step organic Rankine cycle. The study first introduces a new two-step system to recover heat lost from the engine coolant fluid and the exhaust gas at the same time. The working fluids used were water, R-134a and R-123. The total power produced and the efficiency of exergy were set as the objective functions with the aim of optimizing them. The design variables were the pressure in the first and second step of the cycle, the isentropic performance of the pump and the expander, and the temperature of the exhaust gas after recovery of waste heat. It was found that R-123 generated 468kW of total power with an exergy efficiency of 21%, making it the best working fluid under the considered conditions. A sensitive study was also conducted on the improved design to pinpoint the component that effects the performance of the organic Rankine cycle the most.

Ebrahimi and Ahookhosh [25] proposed a new cycle for joint output of Collin heating and power in a micro scale. The cycle consists of a micro organic Rankine cycle, a micro-gas turbine, heat recovery equipment and steam ejector refrigeration cycle. A function named integrated energy-exergy was suggested to increase the efficiency of the cycle by utilizing genetic algorithm. The study found that the integrated model for optimization was better than working on energy and exergy optimization separately. Sensitivity analysis showed that the system was mostly affected by the cooling cycle conditions such as ejector compression ratio, evaporator temperature and organic Rankine cycle steam pressure at the turbine outlet. The recuperator and the combustion chamber had the most exergy loss as they account for 80% and 92% exergy wastage respectively, both in winter and summer. In ideal conditions, minimum pinch point temperature differences of 36°C and 28°C were accomplished in winter and summer. The study showed energy saving of 37% and 28% in summer and winter settings of the cycle, respectively. Total efficiency of 78% and cycle exergy efficiency of 37% is reachable in the summer. Exergy efficiency is greater in winter, 44%, as the compression energy of the cooling cycle is not required.

Benato, Stoppato, Mirandola and Del Medico [26] studied the working fluid choice and plant layout augmentation of an organic Rankine cycle that retrieves the exhaust gases heat content of a 65kW micro-gas turbine. Various plant settings were examined such as subcritical or transcritical and regenerative or simple. The economic and exergetic efficiency of the optimized system was also assessed. An off-design examination was also performed using Aspen Plus, to select the most appropriate organic Rankine cycle and study its activity. Embracing an executive approach that keeps the turbine inlet temperature constant, the best off-design performance was achieved with the working fluid cyclopentane.

Aziz, Mudasar and Kim [27] demonstrated the optimization of organic Rankine cycle systems with high temperatures, in order to allow for selection of the best working fluid and design conditions. Working fluids with high critical temperatures, namely propylcyclohexane, m-xylene and decane, were used. The proposed model tends to be the application of biomass because of the high heat content present when its combustion happens. Non-dominated sorting genetic algorithm was used to perform system optimization, by applying it to conditions such as exergetic efficiency in order to find the maximum work and overall heat transfer requirement to get an estimate of the heat transfer area and the overall cost of the system. The conditions put under limitations for optimizing the performance were degree of superheating, evaporation pressure and pinch point conditions at the heat exchangers. The result was that a 22.9% rise in the overall heat transfer requirement was seen for propylcyclohexane whereas a 45.5% rise was seen for decane, when compared to m-xylene. It was observed that m-xylene had the best exergetic efficiency values, making it the best option from an economic and thermodynamic point of view. The minimum and maximum values of total heat transfer requirement and exergetic efficiency, respectively, were used to find the best evaporation pressure range. There was found to be a small fall in both of these functions, in the presence of an increase in the degree of superheating. The total heat transfer requirement decreased with an increase in pinch point value, which points to lower cost and smaller areas of heat transfer, with low exergetic efficiency; therefore, a pinch point of 8-10 °C was suggested.

Morrone, Algien, Castiglione, Perrone and Bova [28] studied the efficiency of a new biomass - wind energy integrated model for combined heat power generation for

small scale operations. The model was based on organic Rankine cycle integrated with a wind turbine and fed with biomass. The organic Rankine cycle and wind turbine systems worked in parallel to create electrical energy and a backup boiler was set up to give thermal energy in-case the combined heat and power production was low. An initial test was done to determine the right size of the wind turbine. Then, the examination focused on the integrated model, with an in depth look at its use in the residential sector. It was observed that by decreasing the biomass usage and overcoming the intermittence of the wind source, total conversion efficiency was increased with the use of the integrated system. They also suggested that the organic Rankine cycle could be turned off when there is enough wind power to produce the required amount of energy.

Nawi, Kamarudin, Abdullah and Lam [29] studied the possibility of waste heat recovery from the exhaust of marine diesel engines using bioethanol from various microalgae as the working fluid though organic Rankine cycle. The study also takes a look at the thermal efficiency of the model and the pinch temperature of the plant. Microalgae Synechococcus PCC 7002, Chlamydomonas fasciata Ettl and Dunaliella tertiolecta were used as bioethanol producers due to their high yield of production. Maximum total energy produced and greatest system thermal performance were selected as the evaluation criteria to choose the microalgae with the best results. The study found that Synechococcus PCC 7002 had the greatest efficiency of 2.28% for exhaust gas mass flow rate of $4189\,\mathrm{kgh}^{-1}$, while the total power produced was approximately 5.10kW.

Wang et al. [30] compared four forms of organic Rankine cycles with dynamic computational models created in SIMLINK, to study the outcome of part load performance. The four models used were: Organic Rankine cycle with high temperature working fluid toluene directly heated with exhaust condensing at high and low pressure, organic Rankine cycle with low temperature working fluid R245fa with a medium heat transfer cycle and finally the double staged organic Rankine cycle. Comparison of the three models with regards to characteristics such as condensing condition, evaporating pressure, system structure and working fluid were tested on part load performance. The study found that models that matched best with the heat source had good part load efficiency and worked well under design conditions.

Anvari, Taghavifar and Parvishi [31] suggested a combined heating, cooling and power cycle, that contains heat recovery steam generation cycle, gas turbine and absorption refrigeration cycle. The integrated model was put through thorough thermodynamic and exergoeconomic testing. Results showed that combing heat recovery steam generator cycle, gas turbine and regenerative organic Rankine cycle led to 2.5% rise, and adding absorption refrigeration cycle to the gas turbine, regenerative organic Rankine cycle and heat recovery steam generator led to 0.75% rise in the exergetic performance of the whole cycle. Furthermore, from the overall cost of the trigeneration cycle, only 5.5 and 0.45% came from regenerative organic Rankine cycle and absorption refrigeration cycles, respectively.

Li et al. [32] presented a new direct steam generation solar power model, established on cascade steam organic Rankine cycle, steam screw expander and two stage accumulators. Nine organic fluids were used to test system efficiency of the system in seven regions around the world. Results showed that the low temperature accumulator implemented in this model had a greater storage capacity than the usual single stage accumulator, i.e. 1.0 MWhe to 8.4 MWhe.

Patiño and Rivera [33] studied the energetic and environmental outcome of a natural gas combined-cycle power plant combined with post combustion carbon capture and organic Rankine cycle, as a substitute to raise total power output by adding thermal integration between these three processes. The study involved computation of total power output and global warming potential as a function of the level of carbon dioxide picked up. A case control was set in the form of an organic Rankine cycle that produced a significant amount of energy with a stream of hot water to vaporize the working fluid. Then, three cases were tested. Firstly, natural gas combined cycle, post combustion carbon capture and organic Rankine cycle had a total energy rate output of 381.2 MW with 42.43 kg/s carbon dioxide captured and a production of 2.02 MW in the organic Rankine cycle with a global warming potential of 94.75 g CO_2/kWh. The second case had exhaust gas circulation, in which the total power produced was 386.52 MW with 1.905 MW being made in the organic Rankine cycle. Case three combined a post combustion carbon capture and a natural gas combined cycle with total power output of 391.42 MW. The study set an objective framework for practical use to help aid system operation in the future.

Helvaci and Khan [34] conducted a thermodynamic simulation and modeling analysis of a saturated organic Rankine cycle containing flat plate, stationary solar collector. The solar collector was used as a vapor generator, a pump, a water cooled condenser and a vane expander. Twenty- four organic thermofluids were tested. The organic fluids were put through a simulation in which they were exposed to constant condensing pressure and temperature, as well as different cycle pressure ratios. The study focused on the effect the fluids' physical characteristics and pressure ratios on the solar organic Rankine cycle efficiency and their individual effects on aspects such as toxicity, flammability and global warming. The study found that for each working fluid, pressure ratio of the cycle led to different functioning conditions like collector pressure, which in turn resulted in different expander, collector and cycle efficiency. The study also found that 1-butene, when used in the suggested system, gave thermal efficiency of 9.64% and maximum total system output of 210.45 W. R1234ze, RC318, R236fa, R227ea, Neopentane, R601a, R601, R600a, R600, cis-2-butene and trans-2-butene, shoed good solar organic Rankine cycle efficiency. The global warming caused by hydrofluorocarbons and perfluorocarbons, and the flammability of hydrocarbons decrease their range of use. R1233zd, R1234ze, RE245fa2 and RE347mcc appear to be alternative working fluids, although their performance or total energy output was not outstanding. The study presented guidelines to help select thermofields in order to get the best performance in solar energy production while keeping the environmental damage in mind.

Yang et al. [35] studied different working fluids pumps and their compatibility with organic Rankine cycle when using R245fa as the working fluid. Pumps tested included roto-jet pump, hydraulic diaphragm metering pump and multistage centrifugal pump. The effect of outlet pressure and mass flow rate on each pump was studied. Furthermore, the effect of each pump on system exergy destruction rate, thermal and exergy efficiency, back work ratio, total power output and heat absorption rate was analyzed. Results showed that in outlet pressure ranges between 0.4 - 1.1 MPa, maximum efficiency of each pump can go to 30.51%, 55.26% and 58.76%, respectively. There was a measurable difference between the computational and practical back work ratio, which meant that pump power could not be ignored and lesser pump performance had a direct effect on the total power output of the organic Rankine

cycle. Moreover, working fluid pump selection greatly effects the heat absorption rate. Therefore, the study also sheds light on pump selection for organic Rankine cycles with various heat capacities.

2.2 Parabolic Trough Solar Collectors and Applications

Yilmaz and Mwesigye [36] assessed the literature available on parabolic trough solar collectors concerning modeling approaches, thermal and optical efficiency and possible improvements to the existing design. They presented the steady and transient heat transfer examination of single and double phased steam flows and examined the calculations used to understand the physics of parabolic trough collectors. They also exclusively analyzed aspects such as nanoparticle laden flows, augmentation of passive heat transfer and novel design, in studies performed on improving the efficiency of parabolic trough solar collectors.

O'Keeffe, Mitchell, Myers and Cregan [37] proposed an analytic solution to the three dimensional model of the ability of a nanofluid- based direct absorption parabolic trough solar collector under a turbulent flow system. The design consists of a radiative conveyance equation showcasing the generation of radiation through a nanofluid, and a partial differential equation differential equation illustrating the conservation of energy. It was discovered that the usage of dimensionless form creates four controlling dimensionless numbers, three of which portray heat loss to the surroundings, and one denotes the corresponding importance of conduction. The study shows that the increase in temperature of the nanofluid is constant, as it runs through the solar collector. The solution derived from this aids the exploration of the collector's efficiency and helps to calculate design parameters such as the solar absorption characteristics of the fluid, the solar concentration ratio, particle loading, particle type, the inlet temperature and receiver dimensions more accurately. Deeper analysis of the efficiency of the collector uncovers a discrepancy that establishes if it is wise to include a heated-mirror in the solar collector's design.

Mwesigye, Yılmaz and Meyer [38] examined the mathematical aspect of energetic and exergetic efficiency of a parabolic trough solar collector with the use of single walled carbon nanotubes (SWCNTs)-Therminol® VP-1 nanofluid. The thermophysical features of single walled carbon nanotubes were used as functions of

nanotube diameter, nanotube length and temperature, and the properties of Therminol VP-1 were taken to be reliant on temperature. A fluid dynamics processing tool which was based on a fixed volume and the viable k-ε model combined with augmented wall treatment, was used for turbulent modeling. This processing tool received a heat flux profile from the Monte Carlo ray tracing, using the defined parameters. The study demonstrated that there was no significant rise in thermal efficiency, despite better heat transfer performance with single walled carbon nanotubes.

Marefati, Mehrpooya and Shafii [39] assessed the solar energy potential utilizing parabolic trough collector in four different cities in Iran with varying weather conditions. The study looked at aspects such as incident angle correction factor, collector mass flow rate and concentration ratio. It also gauged the effect of input fluid flow rate, aperture area of the collector on the output of the system and fluid inlet temperature. The authors demonstrated the significance of using nanofluids as heat transfer fluid. The study found that Shiraz was the greatest region for effective usage of solar concentration systems, with a useful energy output of 213kWh/m2 per annum and a mean thermal efficiency of 13.91% per annum.

Bioucas [40] used a scaled solar collector model to examine various heat transfer fluids under set conditions, namely: 1000W halogen lamp as the source of radiation. Real time calculations were performed with a multiplexer. Three different concentrations of nanographene (1.15, 0.08 and 0.10 wt%) were tested in a mixture of ethylene glycol 30% and water. The study found increased efficiency of the solar collector. The use of low concentration of nanomaterial resulted in no visible clogging issues.

Singh and Mishra [41] compiled a comprehensive report on the energy and exergy of power plants combined with Solar Parabolic Trough Collectors. Power was produced using supercritical CO_2 cycle as the topping cycle and Organic Rankine Cycle as the bottoming cycle, combined with Solar Parabolic Trough Collectors. Five parameters of exergy were applied, namely: rate of exergy destruction, ration of fuel depletion, irreversibility ration, exergetic efficiency, and improvement potential. Low temperature bottoming Organic Rankine Cycles were applied to five organic fluids: R245fa, R1234ze, R407c, R134a and R1234yf. The study revealed improvement of

thermal and exergetic efficiency of all cycles put together when the normal irradiance rises from 0.5 kW/m^2 to 0.95 kW/m^2. R407c combined cycle was found to have the greatest exergetic and thermal efficiency of:78.07% at 0.95 kW/m2 and 43.49% at 0.95 kW/m^2. R134a and R245fa showed no significant difference. The study revealed that supercritical CO_2 evaporator and turbine has energy destruction of around 9.72% and 8.54% of the inlet exergy, which makes almost 38.10% of the total destruction of exergy in the R407c combined cycle. The study concluded that R407c combined cycle has a low flued depletion ratio of 0.2583 for a solar collector and has the greatest power production of 3740 kW.

Abdulhamed, Adam, Ab-Kadir and Hairuddin [42] conducted a geometric analysis that incorporated the thermal facet of the parabolic trough collector system, transfer of heat, and a way of optimizing the thermal efficiency on the parabolic trough collector receiver. The study included the history and evolution of parabolic trough collectors, different uses of the solar powered parabolic trough collectors, heat transfer efficiency and an analysis of their general performance.

Bhowmik and Amin [43] introduced a novel technology to improve the efficiency of solar thermal collectors. Solar reflector was used with the solar collector to concentrate the diffused and direct solar radiation towards the collector. The reflector was set to change its angle depending on the time of day, in order to get the most out of it. Radiation collected from the sun was converted to heat, which was transferred on to the working fluid for this case water. The model was tested on a prototype and results showed a 10% increase in collector efficiency with the addition of the reflector.

Eryener, Hollick and Kuscu [44] expressed the functional principle and thermal performance of a new solar updraft tower model, which contains of transpired solar collector. The study was conducted on a test model of transpired solar collector by measuring collector cavity temperatures, solar radiation, chimney velocities and ambient temperature during winter and summer seasons. The study found that transpired solar collector efficiency was between 60% and 80%. On a typically sunny day, the greatest temperature increase in the collector area was found to be 16-18°C. The transpired solar collector system was found to be three times more efficient than

the commonly used solar tower glazed collectors. The transpired collector also cut the space needed for solar collector towers in half.

Zou, Li and Wu [45] conducted a modal examination of a trough solar collector. The ANSYS software was initially used to create a finite element model of the collector, in order to find out the mode shapes of trough solar collector surface at various pitch angles as well as the natural frequencies. Natural dynamic features of a model of the trough solar collector were obtained by taking field measurements. The data collected from the first and second steps was used to corroborate the practical applicability of the finite element model. A systematic design approach was used to identify the best measuring taps. The study then established the interrelationship of mode shapes between the measurement and the finite element. The study found that the natural frequencies of the collector are arranged closely, and the results of the finite element simulations correspond to the natural dynamic features that were measured under different pitch angles. Therefore, finite element design is applicable to trough solar collectors. The primary benefits of this study include: finding that inherent dynamic properties of the trough solar collector can be attained using the finite element modal analysis and modal test in field measurements and verifying the exactness and applicability of the finite element design of the channel condenser. This is not to forget that the data collected in this thesis can be used for future analyses such as wind-induced response dynamic analysis.

Hoseinzadeh, Kasaeian and Behshad Shafji [46] conducted a geometric examination of parabolic trough solar collector at various sized of the main parts of the model. The two main characteristics in geometric augmentation of performance of the parabolic collector are the optical efficiency and the rate of the local concentration ratio on the receiver tube. In this study, the collector aperture width, receiver diameter and rim angle were the design characteristics that were upgraded for various sizes of parabolic trough solar collectors. The Monte Carlo Method was used in MATLAB to conduct this analysis by creating coding for the optical and geometric modelling compatible with MATLAB. A lab scale parabolic trough solar collector was studied. Results showed that optical efficiency of 65% was achieved where collector aperture width was 0.6m, receiver diameter was 0.25m and rim angle was 100°. Optical

efficiency of 61% was achieved where the rim angle was 90°, aperture width was 0.7m and receiver diameter was 0.025m.

Xu et al [47] introduced a mathematical model for thermal performance of parabolic trough solar collectors while keeping several factors in consideration such as absorber emissivity, gas in the evacuated annulus, heat transfer fluid, glass envelope and the wind temperature and speed distribution of the absorber. The computed data was then tested on a lab scale parabolic trough solar collector which was usable in solar thermal power plants. The measured and predicted temperatures of the heat transfer fluid at the outlet were found to coincide well. The proposed method was used to perform parametric analysis for the influencing factors. These factors included the wind speed from 2m/s to 12 m/s, the emissivity of the absorber from a measured basis to four times that, the pressure of the H^2 or air from 0.01 Pa to $1x10^5$ Pa and the distribution of temperature with or without the concentrating solar flux. Various conclusions were made in turn by studying how each of these factors effected heat losses and the overall efficiency of the system under set conditions.

Arun and Sreekumar [48] studied the use of a parabolic trough solar collector in a water desalination setup with an integrated tracking system that can track sunlight and change angles accordingly. Parabolic trough collector with north-south alignment facilitated the desalination. The saline water inside the receiver tube was heated and created steam, as the solar irradiation was concentrated towards a focal line in the receiver tube of the parabolic trough solar collector. Steam condensed in the condenser and potable water was formed at the condenser outlet. During this study, the use of various materials for the receiver tube was also tested; these included glass covered copper tube and stainless steel tube. The study found that the efficiency of the parabolic trough solar collector was dependent on the focal receiver and tracking of sunlight. Chemical and physical investigation of desalinated and saline water was done. The desalination setup had 2 litre/m2 of output.

Marrakchi, Leemrani, Asselman, Aoukili and A. Asselman [49] studied the three dimensional distribution of temperature of the absorber tube in parabolic trough solar collector. This was done by observing the outcome of applying uniform solar heat on a parabolic trough solar collector. COMSOL Multiphysics 5.1 was used to conduct this study. Solar heat flux condition of 1000W/m2 was used as the input data to conduct

the three dimensional analysis of temperature distribution. The study found that the cover and fluid temperatures increase continuously from 298K to 318K, which is the specific temperature equilibrium value.

Batuecas, Mayo, Díaz and Pérez [50] tested the environmental effects of two variations of molten salts and synthetic oil in order to find out whether salts are better than synthetic oil from an environmental viewpoint, by using the life cycle assessment methods. The life cycle assessment demonstrated higher impacts in case of the synthetic oil as compared to the molten salts.

Heidsieck, Dörrich, Weidner and Rieger [51] studied the use of polysiloxanes as heat transfer fluids, as they have great resistance to high temperatures. The polymers were exposed to a thermally induced equilibration reaction that leads to changes in physical characteristics in the heat transfer fluids generally used. The study found that, based on the selected model compounds, branched siloxanes have great resistance against thermal equilibration reaction. This paper further researched how mixing polysiloxane with industrial used fluids such as Therminol VP-1 and Syltherm 66 effects the thermodynamic, chemical and physical properties of the mixture. Also the mixtures resistance to high temperatures and cycles of heating and cooling effect on the thermal properties of the mixture is assessed. It was shown that using a 5% mixture of polysiloxane with Therminol VP-1 improved the thermal conductivity of the system by 7%.

2.3 Power Generation

Suresh, Thirumala, Rao and Ramaswamy [52] proposed a detailed methodology to design the size of solar field for a parabolic trough plant which includes thermal storage and hybridization. The size of the solar field is optimized for the maximum annual solar to electric conversion efficiency, using the concept of solar multiple (ratio of actual aperture area to the reference aperture area needed to get rated power output at maximum solar input). This procedure is validated with the existing parabolic trough plants (Solar Energy Generating Systems VI and Solana Generating Station); it was found that the annual electrical energy generated by the plant matches reasonably well. Figure 3 represents a schematic of the CSP with TES.

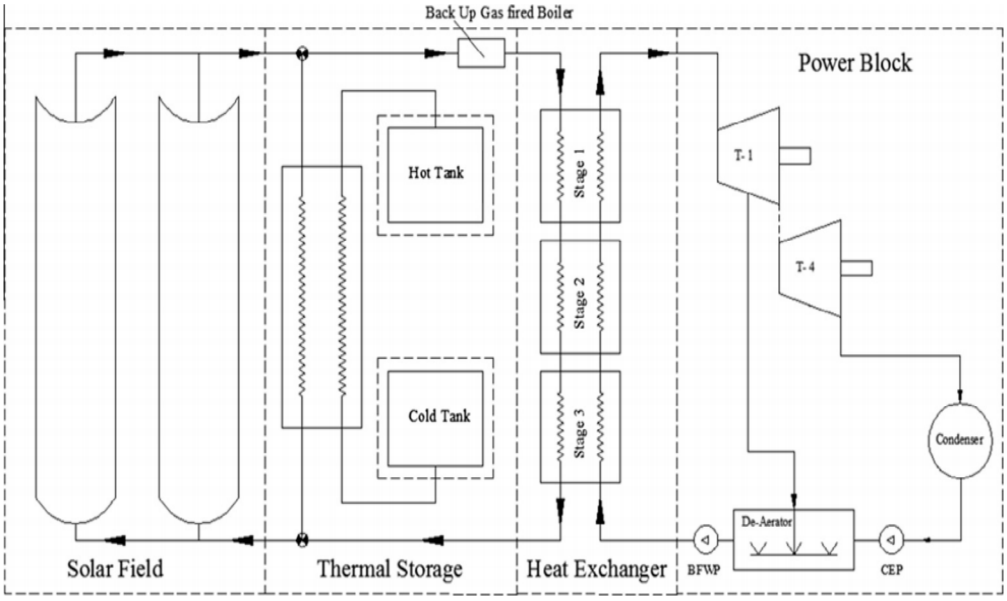

Figure 3: Schematic of a CSP with Thermal Energy Storage [52]

Poghosyan and Hassan [53] conducted a parametric study to determine the size of a thermal energy storage and the solar field size such that the parabolic trough model, Shams-1 UAE, would provide energy throughout the day and night. This thesis is important since the present research will be conducted in the same country and because the theoretical data will definitely be helpful in the process. An interesting data recovered in this thesis is of the monthly direct normal irradiance (DNI) readings in Abu Dhabi. It might be very surprising to observe that the DNI level in October is the highest and in July is the lowest. Figure 4 displays the DNI levels for July and October.

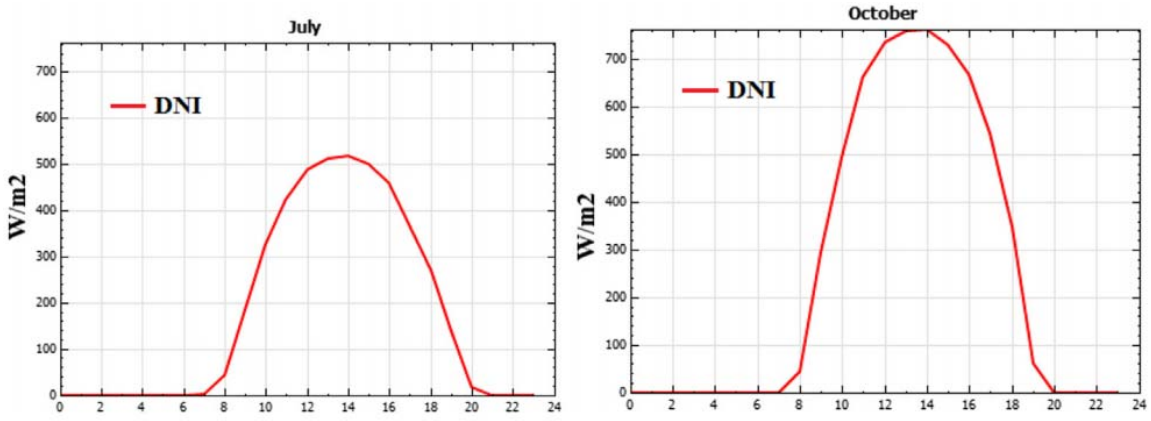

Figure 4: Lowest and highest DNI levels respectively in UAE [53]

Yuanyuan and Zhang et al. [54] assessed two hybrid combined cycle power systems that use solar heat and methanol with carbon dioxide capturing integrated. The high methanol conversion rate allows usage of solar heat at only 200-300 ^{o}C. The proposed solar assisted system carbon dioxide emissions are 36.8% lower, fossil fuel saving ratio of 30% with solar thermal share of 20% as compared to gas steam combined cycle with flue gas carbon dioxide capture system.

Acharya and Bhattacharjee [55] designed a model of wind and solar thermal hybrid power plant with spring storage system. Wind energy is harnessed by a hybrid vertical axis wind turbine; solar energy is produced by a Stirling engine, with the surplus energy being stored in a winding spring. The plant performance has been analyzed of the 2.6kW hybrid power plant model.

Peng, Hong and Jin [56] proposed a solar driven triple cycle in order to generate power during low insolation periods. The triple cycle integrated solar gas turbine top cycle, steam Rankine cycle and the Kalina bottom cycle. The operation strategy was to utilize all three cycles during peak hours, and as the insolation level decreased, accordingly the top gas turbine cycle was bypassed, followed by the steam Rankine cycle, only allowing the Kalina cycle to operate, which requires low temperatures.

Athari, Soltani, Seyed Mahmoudi, Rosen and Tatiana Morosuk [57] assessed energy, exergy and exergoeconomic analyses for a biomass integrated post-firing combined cycle power plant. The energy and exergy efficiencies of the cycle were found to be maximized at specific compressor pressure ratio values, and that higher pressure ratios reduced the total unit product cost. The major cost rate of the power plant configuration was due to the exergy destruction cost rate.

Al-Soud and Hrayshat [58] designed a 50 MW concentrated solar power plant to be used for electricity generation in Jordan, and analysis of its economic feasibility has been performed. An estimate of the energy yield of the plant was computed and it was proposed that the establishment of the plant be in Middle East and North Africa (MENA) region.

Choi, Ahn and Kim [59] conducted a study to simulate a triple combined cycle which blended a gas turbine combined cycle with solid oxide fuel cell system. The

impact of post combustion carbon capture was evaluated. The carbon capture reduced the efficiency of the triple cycle by 5%. Carbon emissions were reduced on average 7 times lower with carbon capture.

Spelling [60] conducted a thermo-economic study on three different hybrid power plant configurations, including both solar thermal and photovoltaic hybridization options in order to assist in decision making. Solar photovoltaic combined-cycle power plants were able to integrate up to 63% solar energy annually, while hybrid gas turbine combined cycle systems provided the lowest cost of solar electricity, with costs only 2.1% higher than a reference unmodified combined cycle power plant.

Gunasekaran, Mancini, El-Khaja, Sheu and Mitsos [61] proposed four integration techniques for advanced zero emissions power cycle with a parabolic trough: vaporization of high-pressure steam, pre heating of high pressure stream, heating of intermediate-pressure turbine inlet stream and heating of low-pressure turbine inlet stream. A comparison of the proposed vaporization scheme with existing hybrid technologies without carbon capture and storage (CCS) showed that it has a higher annual incremental solar efficiency than most hybrid technologies. Moreover, it was shown that the proposed design had a higher solar share compared to hybrid technologies with higher incremental efficiency.

Peterseim [62] investigated 17 different concentrating solar power biomass hybrid configurations in regards to their technical, economical and environmental performance. A molten salt thermal storage was considered for the best hybrid configuration. Results showed that solar tower–biomass hybrids reached, the highest net cycle efficiency, 32.9%. Based on the annual electricity generation, CSP– biomass hybrids had an up to 69% lower investment compared to standalone concentrating solar power systems.

Bombarda, Invernizzi and Gaia [63] conducted analysis on an ocean thermal energy conversion (OTEC) system, with the goal of making it economically viable. A closed cycle system of organic Rankine cycle power plant with multiple modules in series on warm water flow, improvied performance by 30% as compared to a single level cycle. A hybrid solar-OTEC plant was investigated for day and night operation, which would triple the energy produced during daytime at the specified water flow.

Antonanzas, Alia-Martinez, Martinez-de-Pison and Antonanzas-Torres [64] conducted a feasibility study of solar thermal hybridization with parabolic trough technology in 21 Algerian open cycle gas turbines and combined cycle gas turbines, which represented approximately 97% of electricity generation. A yield increase of 24.8 GWh/year and carbon dioxide emissions savings of 9.91 kton/year was estimated to be feasible with solar field sizes ranging from 30 to 37 loops.

Popov [65] proposed a concept of innovative hybridization of gas turbine combined cycle plant and solar power system. A mechanical chiller was added for complete cooling of gas turbine inlet air. The chiller was powered by electricity generated from a dedicated photovoltaic plant. Another proposed option was an absorption chiller. The steam for this chiller was generated in a solar field equipped with linear Fresnel reflectors. This concept offered an effective way for further implementation of compact linear Fresnel reflector technology.

Ghasemi, Sheu, Tizzanini, Paci and Alexander Mitsos [66] developed a model for an existing organic Rankine cycle using low temperature geothermal brine. The system was validated with a set of 7200 operation data collected in one year. The system was also retrofitted with low temperature solar trough system. The hybrid system showed higher seconds law efficiency (up to 3.4%) compared to combined individual geothermal and solar system.

Peterseim, White, Tadros and Hellwig [67] conducted an assessment to identify the most suitable concentrated solar power technologies to hybridize with Rankine cycle power plants, using both conventional and non-conventional fuels. The findings of the study showed that Fresnel systems are the best technology for feed-water preheating, cold reheat steam and less than 450 ℃ steam boost applications. Parabolic troughs which had thermal oil ranked second for all solar power plant with steam temperatures less than 380 ℃. For steam temperatures above 450 ℃, the solar towers with direct steam generation scored higher than solar towers using molten salt and the big dish technology. At and above 580 ℃ the big dish was the only alternative to directly provide high pressure steam.

Corona, San Miguel and Cerrajero [68] quantified the sustainability of concentrated solar power plant and analyzed how this was affected by hybridization

with different natural gas inputs. A sensitivity analysis was conducted on a 50 MWe concentrated solar power plant in order to evaluate the environmental performance of the plant operating with different natural gas inputs. It was observed that the utilization of natural gas had an overall negative effect on the environmental performance such as climate change, natural land transformation, fossil fuel depletion and terrestrial acidification.

J.-F.Hoffmann et al. [69] analyzed the thermophysical features of seven vegetable oils, namely thermal conductivity, specific heat capacity and density along with the rheological characteristic of dynamic viscosity. The aim of the study was to find how these properties are altered at different temperatures, ranging from room temperature up to 250 °C. The study found that the change the characteristics being studied were altered by the fatty acid content in the oils, while all the properties being analyzed did show an increase with rising heat.

Andrey Yasinskiy et al. [70] studied the physical and thermal properties of titanium dioxide based nanofluids, including density, viscosity, stability, and heat transferability. The study found that using titanium dioxide nanoparticles alongside 1-octadecanethiol greatly augmented heat transfer in concentrating solar power plants. The density and viscosity were found to have a small rise of 0.12% and 4.85%, respectively, while a greater increase was seen in isobaric specific heat (52.7%) and thermal conductivity (25.8%). The titanium dioxide nanoparticles demonstrated a 35.4% rise in efficiency when compared to pure heat transfer fluids, making them a favorable substitute to the heat transfer fluids in concentrating solar power plants.

Yunus and Yüksel [71] studied the use of modified organic Rankine cycle combined with parabolic trough collector to create hydrogen. The components of the model being studied include a modified organic Rankine cycle, a parabolic trough collector, a Proton Exchange Membrane electrolyzer and a single effect absorption cooling system. Electricity was created by the input of heat energy, and sourced by solar energy, into a modified organic Rankine cycle. Such electricity was then applied to the formation of hydrogen. The study analyzed the effectiveness hydrogen production, using this modified system and found that solar radiation was a major factor in determining exergy efficiency and formation rate of hydrogen, with a rise of 58% -

64% in exergy efficiency with a 400 W/m^2 to 1000 W/m^2 rise in solar radiation; the same increase in solar radiation led to a rise in formation rate from 0.1016 kg/h to 0.1208 kg/h.

Bellos and Tzivanidis [72] designed a system that has the ability to maximize electricity output by the use of waste heat in a solar powered hybrid organic Rankine cycle. The parabolic trough collectors were linked to a storage tank, that supplied the heat recovery system, which also used waste heat at low temperatures of 150℃ - 300℃. The study investigated four different working fluids, MDM, toluene, cyclohexane and n-pentane in the modified organic Rankine cycle model. The study found that toluene showed the highest formation of electricity, followed by cyclohexane MDM and pentane. For the given temperature range of the waste heat, electricity production with toluene was documented as being between 479kW and 845 kW and the model efficiency between 11.6% and 19.7%. The study also demonstrated that the higher the temperature of the waste heat source, the greater the amount of waste heat received by the organic Rankine cycle for all the working fluids tested.

Mauro and Reiset [73] studied ways of improving the total thermal efficiency in a floating production storage and offloading platform, by finding different methods to reuse waste heat and meet the need for hot water in order to get the most out of electricity generation through the organic Rankine cycle. The authors aimed to simultaneously decrease the carbon footprint of the system. Flue gasses from the gas turbines were used in the organic Rankine cycle and cogeneration system, experimenting with a simple and a regenerative cycle setting. The organic Rankine cycle and water heating systems were designed with the curves of the GE LM2500 and GE LM2000 turbines. The design was computed using a genetic optimization method, while considering the decrease in fuel consumption, decline in CO_2 emission and cost of the organic Rankine cycle. The study showed that reusing the waste heat provided up to 21% of the total electricity required. This improved the efficiency of the model by 10.8% and increased usage factor by 19.2%. The study also demonstrated a 22.5% decrease in fuel usage and CO_2 production during the lifespan of the floating production storage and offloading platform.

Jahar Sarkar [74] proposed a new design to increase the efficiency of subcritical and supercritical organic Rankine cycles for the greatest heat recovery. The design had the capability to estimate pinch point locations in evaporator and condenser concurrently, which was done by pressure optimization, by improving the working fluid mass flow rate to attain the highest possible heat recovery efficiency using certain working fluids. The selection of the working fluids was based on environmental and thermodynamic criteria such as thermal efficiency, irreversibility, exergetic efficiency, turbine size parameter, net work output and heat transfer requirement. The study found that ammonia was the greatest with regards to lesser mass flow rate required, decreased turbine staging and size and higher exergetic efficiency. Isopentane was found to be better at heat recovery efficiency and high power output.

Katulić, Čehil and Schneider [75] computed a system in which heat exchangers may be arranged in serial or parallel at different pressure levels in a heat exchanger network, which is made of several pressure levels, and a re-heater that utilized working organic fluids at lower levels of pressure. They performed exergoeconomic augmentation by focusing on the functioning parameters of the working fluids at different pressure levels and the layout of the heat exchanger. The aim of the study was to decrease the cost of investment and loss of exergy in the bottoming cycle of the heat exchanger network, with the use of gradient optimization and genetic algorithm. The study demonstrated the potential to decrease the cost of destroyed exergy by utilizing organic fluids at lover pressure levels and working on the layout of the heat exchanger.

Cocco, Petrollese and Tola [76] studied the usage of concentrating solar technologies to provide power and heat for industrial processes. Three heat and power generation sections were assessed. Power was generated using an organic Rankine cycle while heat was provided by a heat generator either parallel or downstream to the organic Rankine cycle system by recovering the heat lost by the organic Rankine cycle. The system's exergy efficiency was used as a measure to determine the best configuration. Various power-heat ratios, formation of hot water and saturated steam were taken into account. The study found that using a heat generator parallel to the organic Rankine cycle is the best way to provide high-pressure steam, whereas it is better to pace it downstream to the organic Rankine cycle for low-pressure steam and high power-heat ratios. Using waste heat from the organic Rankine cycle is a viable

option for the production of hot water only if full heat can be used, in order to avoid great exergy loss.

Toghyani, Baniasadi and Afshari [77] studied the outcome of using an organic Rankine cycle, combined with a parabolic trough solar system and a thermal storage system, in a simulation based on four Nano-fluids in the solar collector system. The Nano-fluids used were Al2O3, SiO2, CuO and TiO2. The second law of thermodynamics was applied to investigate the impact of dead state temperature, volume fraction of the various Nano-particles and solar intensity on the efficiency of the integrated model. The genetic algorithm was also used to increase the efficiency and total power produced by the organic Rankine cycle. A two -tank system was used to store solar thermal energy, to further optimize energy output when sunlight was not present. Finite Time Thermodynamics was used to assess the efficiency of the thermal energy storage and solar collector system. The study found that greater fractions of Nano-particles and higher dead state temperatures resulted in higher exergy efficiency. Greater solar irradiation led to more power output. Furthermore, CuO oil was the Nano-fluid that was found to have the best outcome exergetically.

2.4 Thermal Energy Storage Applications

Sivapalan et al [78]. conducted experiments to figure out the ideal amount of paraffin wax in water- paraffin wax nanoemulsions, to be utilized as media to store thermal energy. Multiple concentrations of water- paraffin wax nanoemulsions were tested, with the width of dispersed phase varying from 200 – 600nm. The experiment showed a corresponding increase of the specific heat of the nanoemulsions as the concentration of paraffin wax increased. A decrease in the viscosity of the emulsion was seen at higher temperatures. The efficiency of the water- paraffin wax emulsions as well as pure paraffin wax and water were tested in the charging cycle of thermal energy storage. The Tests revealed that the water- paraffin wax emulsion with a paraffin wax concentration of 10% had the greatest amount of energy stored per unit time per unit heat exchanger volume, which surpassed the performance of pure paraffin wax and water by 23% and 10% respectively.

Fang, Niu and Deng [79] introduced an index of effective energy storage ratio, Est , in order to define the effective energy storage capacity oh a Latent heat thermal

energy storage system in comparison to an optimal stratified water storage system of equal volume. A combined arithmetical heat transfer and fluid flow technique was first verified and then utilized to establish the Est of a tube-in-tank design. The impact of effective thermal conductivity on the effective energy storage ratio was shown. It was demonstrated that there is an ideal compactness factor for phase change material at any finite value of effective thermal conductivity, and that the ideal compactness factor and the analogous highest effective energy storage ratio are greater for phase change material at a higher effective thermal conductivity. They also demonstrated that a large portion of the theoretical energy storage capacity is not being used even at the ideal compactness factor for phase change material at any effective thermal conductivity. This shows that heat transfer improvement in relation to the fluid may further improve the effective energy storage ratio.

Alva and Lin [80] published a review of some elements of thermal energy storage, which include the function of thermal energy storage in various thermal energy sources and its impact on decreasing the need for using fossil fuels. Generating solar energy, creating thermal comfort and other functions of thermal energy storage are discussed. They also discussed multiple categories of thermal energy storage materials for their cost, physical properties, appropriateness to different applications and performance. They also looked closely at the categories of thermal energy storage systems available.

Ward and Teprovich Jr. [81] illustrated the cost effectiveness of using CaAl2 as a thermal energy storage material. They found that CaAl2 works at 600 °C and has great reversibility, equilibrium pressures that are practical for thermal energy storage systems that are metal hydride based, as well as having acceptable thermal conductivity. They found that the hydrogenation of CaAl2 happens in two steps to produce Al and CaH2, and is dehydrogenated at 600 °C to create CaAl2 by altering the pressure of hydrogen. They concluded that CaAl2 serves as the most cost effective metal hydride thermal energy storage material with the ability to work at or above 600 °C.

Nandi and Bandyopadhyay [82] created an arithmetic model to study packed bed thermocline thermal energy storage. The transport model was established on a macroscopic variation of the K– ε formula for turbulent flow conditions. The multi-

dimensional transport methods were considered under different flow settings and the effectiveness and features of the operation were tested in various geometrical and operational conditions at a fixed thermal energy storage size of 50 MWh for the charging and discharging mechanisms. They also studied the outcome of changes in criteria like aspect ratio, porosity, Reynolds number of inlet fluid, and filler size on the performance of the thermal energy storage. The ideal geometry and condition of the thermocline thermal energy storage system were established by the Taguchi – computational fluid dynamics combined method. The study found that the aspect ratio and porosity were the most essential design criteria for thermocline thermal energy storage.

Nyamsi, Lotototskyy and Tolj [83] used the first law of thermodynamics to design and examine thermal energy storage systems using metal hydrides. The metal hydrides tested were Mg, LaNi5, Mg2FeH6 and Mg2Ni. The comparative parameters used were energy storage performance and volumetric energy storage. The effect of opertational settings such as heat transfer, hydrogen pressure, temperature and fluid mass flow rates as well as reactor model, on the comparative parameters were analyzed. Initial results demonstrated that Mg hydrides stored energy between 1.3-2.4 GJ m−3, whereas energy storage can be reduced to as much as 30% because of their slow intrinsic kinetics. In contrast, combining Mg hydrides with LaNi5 led to heat recover at a temperature greater than 330K with low energy density ca.500 MJ m−3, granting favorable functioning conditions. The results of this analysis could be useful in finding hydrides for heat storage applications

Lugolole, Mawire, Lentswe, Okello and Nyeinga [84] presented the outcome of analyzing and comparing three sensible heat storage systems during charging cycles with three flow rates of 4 ml/s, 8 ml/s and 12 ml/s respectively. An oil only storage tank was compared with two storage systems that used sunflower oil for the heat transfer fluid with particle diameters of 10.5mm and 31.9mm. The large pebbles thermal energy storage system charged up the slowest because of its lesser thermal mass. The fastest to charge was the oil storage system followed by the small pebbles thermal energy storage system. The small pebbles were able to reach thermal equilibrium faster than the large pebbles, and thus have a faster rate of increase in temperature. The big pebbles usually undergo temperature falls. The aim of this study was to demonstrate the thermal

efficiency of pebble packed beds that used sunflower oil as the heat transfer fluid in medium ranges of temperature, in order to be used for cooking. The thermal efficiency was analyzed during the charging cycle, using three criteria which were exergy rate, energy rate and stratification number. Small pebbles thermal energy storage systems were found to be the optimal model in term of charging exergy and energy as they produced greater charging energy and exergy rates. It was discovered that the exergy rates were reliant on the difference in temperature between the top and bottom of the storage and the average storage temperature. Exergy rates had no clear connection to charging flow rates. Thermal stratification in thermal energy storage models that use liquid storage materials augment the energy performance. Stratification happens when hotter lower density liquid rises and cold higher density liquid drops to the bottom. The oil thermal energy storage system demonstrated the quickest rise and fall in stratification value because of its lower thermal mass. In general, the slowest rate of fall in the stratification value was observed in large pebble thermal energy storage models for all flow rates. This indicates that better useful energy is stored in large pebble thermal energy storage models despite how it charged up with lesser initial rate. The small pebble thermal energy storage system worked better in view of the thermal efficiency parameters tested in this paper.

Mehrabadi and Farid [85] aimed to introduce a novel salt-based thermochemical compound for long term storage of low grade thermal energy, that could allow passage over the hurdle posed by the mismatch between energy supply and demand. They studied the dehydration performance and energy density of $CaCl_2 \cdot 6H_2O$, $Al_2(SO_4)_3 \cdot 18H_2O$ and $MgSO_4 \cdot 7H_2O$, $MgCl_2 \cdot 6H_2O$, and $SrCl_2 \cdot 6H_2O$. Then, a lab scale packed bed reactor was used to test the best salt, as identified by the evaluation as being the most suitable for storing low grade thermal energy, in two low cost porous host structures, namely expanded clay and pumice. Results revealed that $SrCl_2 \cdot 6H_2O$ had the lowest dehydration temperature and greatest energy density, which means more than 80% of its energy density could be stored at less than 90 °C. Thermal cycling the composites showed that clay-$SrCl_2$ can store up to 29 kWh/m^3 (40 wt%), whereas pumice-$SrCl_2$ can store up to 7.3 kWh/m^3 (14 wt%). The energy produced from the pumice composite was sustained almost constantly over ten cycles, whereas the expanded clay showed a drastic fall in performance after 4 cycles.

Peiró, Gasia, Miró, Prieto and Cabeza [86], compared two commercial heat transfer fluids that are commonly used in different industries and concentrated solar-thermal power plants. The fluids compared were thermal oil therminol VP-1 and silicone fluid Syltherm 800. The data provided by the manufacturers of both these fluids was first reviewed. Then, both fluids were tested in a two-tank molten salt thermal energy storage pilot plant. The study showed that under the same conditions, Therminol VP-1 was better due to its low thermal losses, higher heat transfer and lower energy consumption in the heat transfer fluid pump.

Bozkaya and Zeiler [87] studied the use of night ventilation for energy regeneration, as an alternative to the heat pump and air handling unit, to achieve thermal balance for cooling dominated loads. The cost effectiveness and energy efficiency of both systems was also compared. It was found that night ventilation can decrease power consumption by 19.3 MWH/year, which adds up to 26.4% rise in the model's coefficient of performance.

Schaefer and Thess [88] studied the use of closed energy storage for industrial and household use. A computational study was done on a closed low pressure honeycomb adsorber, which contained layers of stacked honeycomb blocks with heat exchanger plates separating their rectangular channels. The absorption pair used was water and Zeolite 13x. A one dimensional model was used for the single channel honeycomb blocks; the one dimensional equation was made more comprehensive with the use of heat source and sink terms to account for the transversal heat conduction. The mass transportation equation was also adjusted for rectangular channel flow. The study found a significant connection between the adsorption process, head and mass transfer, and that they had to be studied based on their interconnection. They also found that when it comes to modeling, spatial differences in pressure, temperature and local deviation from the equilibrium of adsorption are all important. The study suggested that small changes in rarefaction due to slip should be taken into consideration. As for the practical use of the honeycomb adsorber, performance can be optimized by changing the geometry of the honeycomb model, for example channel size. The local optimum was found to be the outcome of inverse dependencies of the external and internal mass transfer resistance on the channel size. They also found that thermal energy could be controlled well by the inlet pressure.

Baser and McCartney [89] studied a simulation model for transient ground temperatures in a field scale soil borehole thermal energy storage system. The soil borehole thermal energy storage system contained thirteen 15m deep borehole heat exchangers set in conglomerate bedrock, 1.5m apart. Heat energy from solar thermal panels was transferred to the soil borehole thermal energy storage system for 4 months, and then the subsurface was observed for a five-month ambient cooling period. The system was placed above a water table and was relatively dry, so an integrated water flow and heat transfer system was set in place to imitate the ground response. A simulation of a conduction only model for saturated conditions was also tested. It was found that there was a measurable difference in the ground temperature where the heat exchangers were installed. Even though the computational simulations show a permanent fall in the level of saturation, and thermal conductivity happened at the borehole heat exchanger locations.

Yong, Wen and Cheng [90] suggested a new deep underground thermal heat storage model by utilizing single depleted oil well, and the coaxial borehole heat exchanger with insulation, to retrofit the depleted oil well for seasonal thermal energy storage. Initially, a detailed model was created which combined wellbore and formation heat transfer and tested the efficiency of storing heat in the summer and pace heating in the winter. Results showed that inlet temperature has the greatest effect on storage performance. During year long operations a total heat storage for the depleted oil well with a depth of 2000 m was 4.7106 MJ, while the total heat extraction was approximately 2.9×10^6 MJ more than 8×10^5 MJ, which is more than the heat extracted without storage progress. It was suggested that the depleted oil well underground thermal heat storage system could be used to store waste heat in the summer, and that heat could be used for space heating during the winter.

Ward, Teprovich Jr, Lui, He and Zidan [91] studied the use of $CaAl_2$ as a high temperature thermal energy storage medium in concentrated solar power systems. $CaAl_2$ proved to have the ability to perform well at 600°C with good reversibility, equilibrium pressures suitable for metal hydride thermal energy storage models and favorable thermal conductivity. $CaAl_2$ was found to hydrogenate in a two-step process from CaH_2 and Al and dehydrogenate to recreate $CaAl_2$ at 600 °C by changing the hydrogen pressure.

Chapter 3. System Configurations and Modeling

This chapter involves formulating and defining system parameters and design conditions for the Organic Rankine cycle, the parabolic trough solar collector and the overall power generation from the cycle. The thermodynamic properties of the ORC, the thermodynamic and heat transfer analysis of the heating fluid in the PTSC are all discussed in this chapter. In addition, integration of the complete system is also provided.

3.1 Organic Rankine Cycle (ORC) Modeling

ower production for the system will be utilized from the Organic Rankine Cycle in this study. The Organic Rankine cycle has organic fluids as its working fluid, as compared to the conventional Rankine Cycle which uses water as its working fluid. Since the integration of this Organic Rankine Cycle will be with a PTSC, the Organic Rankine Cycle will use a heat exchanger to heat the organic fluid rather than the conventional method of using a boiler that heats the working fluid in a Rankine Cycle. The heat transfer fluid provides thermal energy to vaporize the organic fluid in the heat exchanger or the evaporator. Figure 5 shows the schematic diagram of the simple ORC.

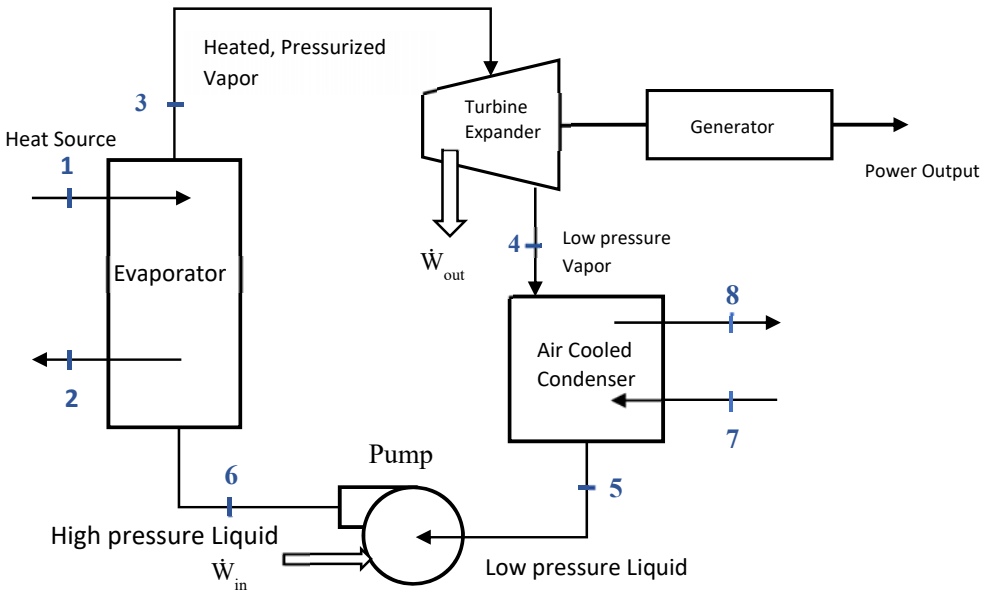

Figure 5: Schematic diagram of simple ORC

The heat transfer fluid transfers the thermal energy it gains from the PTSC to the organic fluid in this process. The vaporized organic fluid is then expanded in the turbine where the pressure is dropped to produce electricity and provide superheated organic fluid at the condenser pressure. The organic fluid then enters the condenser where it is cooled and again pumped into the evaporator.

3.1.1 Evaporator

High pressure organic fluid enters the evaporator in liquid form, where it is heated to vapor form to the required turbine inlet temperature. The heat transfer fluid enters the heat exchanger and leaves as a fluid and transferring thermal energy to the organic fluid. The following equations will be used for modeling equations of the heat exchanger or evaporator.

Mass Balance:

$$\dot{m}_3 = \dot{m}_6 = \dot{m}_{orc} \tag{3.1}$$

$$\dot{m}_1 = \dot{m}_2 = \dot{m}_{HTF} \tag{3.2}$$

where $\dot{m}_{orc}$ is the mass flow rate of the organic fluid and $\dot{m}_{HTF}$ is the mass flow rate of the HTF. Figure 6 illustrates the schematic of the evaporator.

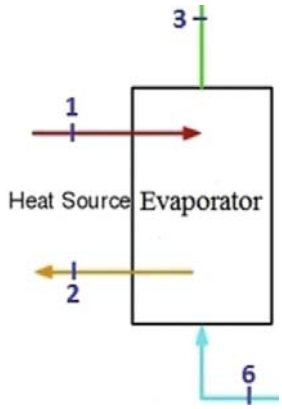

Figure 6: Evaporator schematic

Energy Balance:

$$\dot{Q}_{ev} = \dot{m}_{Orc}(h_3 - h_6) = \dot{m}_{HTF}c_{p(HTF)}(T_1 - T_2) \tag{3.3}$$

$$\dot{m}_{Orc} = \frac{\dot{m}_{HTF} c_{p(HTF)} (T_1 - T_2)}{(h_3 - h_6)} \quad (3.4)$$

3.1.2 Turbine

The superheated vapor state of organic fluid will enter the turbine, giving work output and in turn expanding the fluid to the condenser pressure. Figure 7 is the schematic of the turbine and the modeling equations for the thermodynamic analysis of the turbine.

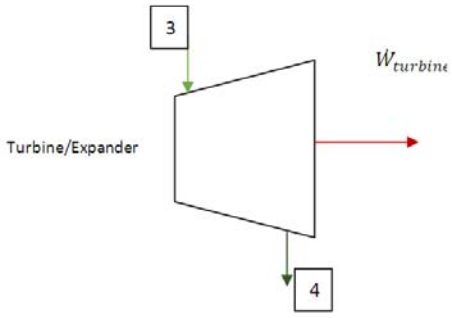

Figure 7: Turbine schematic

Formulation:

a) Mass balance:

$$\dot{m}_3 = \dot{m}_4 = \dot{m}_{orc} \quad (3.5)$$

b) Energy balance:

$$\dot{W}_{turbine} = \dot{m}_{orc}(h_3 - h_4) \quad (3.6)$$

3.1.3 Condenser

The superheated organic fluid is then cooled and condensed in the condenser as heat is transferred to the air that passed through the condenser. Figure 8 presents the schematic for the condenser and the modeling equations for the condenser.

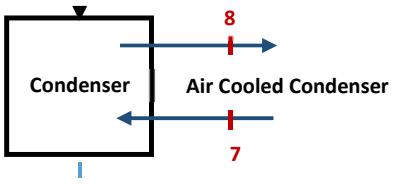

Figure 8: Condenser schematic

Mass Balance:

$$\dot{m}_4 = \dot{m}_5 = \dot{m}_{orc} \tag{3.7}$$

$$\dot{m}_8 = \dot{m}_7 = \dot{m}_{air} \tag{3.8}$$

Energy Balance:

$$\dot{Q}_{cond} = \dot{m}_{Orc}(h_4 - h_5) = \dot{m}_{air}(h_8 - h_7) \tag{3.9}$$

3.1.4 Pump

The ORC fluid leaving the condenser enters the pump, where it is pressurized and transferred to the heat exchanger. Figure 9 illustrates the pump schematic.

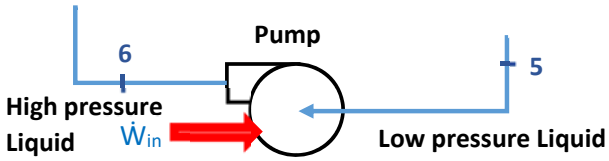

Figure 9: Pump schematic

a) Mass balance:

$$\dot{m}_3 = \dot{m}_4 = \dot{m}_{orc} \tag{3.10}$$

b) Energy Balance

$$h_6 = w_{pump} + h_5 \tag{3.11}$$

$$w_{pump} = v_5 (P_6 - P_5) \tag{3.12}$$

3.1.5 ORC input parameters

Using the system of equations from sections 3.1.1 to 3.1.4, the ORC is formulated on EES software. Each ORC is run for a turbine inlet pressure at 80% of the organic fluids critical pressure in order to achieve considerable cycle efficiency as well as not reaching supercritical conditions for the fluid. The condenser pressure is set at 10 kPa in order to achieve appropriate cycle efficiency and also to keep the condenser intact since further reducing the pressure will cause the difference between the atmospheric and condenser pressure to be high and may allow penetration of atmospheric air into the system and damaging the ORC components critically. All

component efficiencies and isentropic efficiencies are set to 90%. Table 2 lists out the ORC input parameters.

Table 2: ORC input parameters

Parameter	Unit	Value
ORC condenser pressure	kPa	10
ORC pump inlet quality	-	0
ORC turbine inlet pressure	MPa	80% of ORC fluid critical pressure
Pump efficiency	%	90
Isentropic efficiency	%	90
Condenser efficiency	%	90

3.1.6 Efficiency

The thermal efficiency of the Organic Rankine cycle can be computed from the turbine output and the energy input from the PTSC, which can be formulated as the following:

$$\eta_{thermal} = \frac{\dot{W}_{turbine} - \dot{W}_{pump}}{\dot{Q}_{PTSC}} \tag{3.13}$$

The exergetic efficiency of the cycle can be calculated, using the following equation [53].

$$\eta_{exergetic} = \frac{\dot{X}_{out,ORC}}{\dot{X}_{in,ORC}} \tag{3.14}$$

where the exergy input and output of the ORC are modelled as follows:

$$\dot{X}_{out,ORC} = \dot{m}_{orc}[(h_{turbine,in} - h_{turbine,out}) - T_0(s_{turbine,in} - s_{turbine,out})] \tag{3.15}$$

$$\dot{X}_{in,ORC} = \dot{Q}_{PTSC}\left(1 - \frac{T_{amb}}{T_{PTSC,out}}\right) \tag{3.16}$$

3.2 PTSC Modeling

The Parabolic trough solar collector contains solar collectors, receiver and an absorbing tube. The solar collector is manufactured to have a parabolic shape, and its objective is to reflect solar rays towards the absorbing tube. The absorbing tube has absorbing characteristics, as it is made from metal and coated with black paint on its surface to increase heat absorption. Furthermore, the tube is normally lined by a glass cover for reduction of heat loss via convection and radiation.

The model of the PTSC is done by analyzing the collector, receiver and glass cover separately, and then combing the parameters to analyze the energetic and exergetic performances of the PTSC. Figure 10 shows the schematic diagram of a PTSC, and how the rays of sunlight are reflected by the collector onto the receiver.

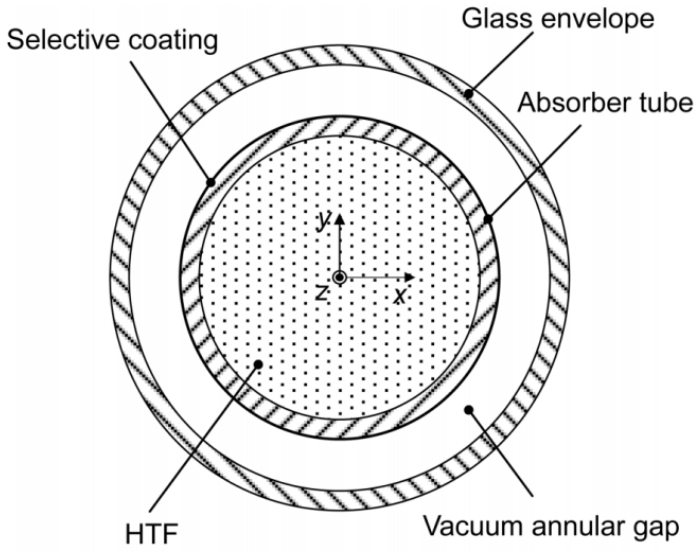

Figure 10: PTSC cross-section schematic [36]

3.2.1 Heat transfer formulation for PTSC

The solar energy that is used by the PTSC is the solar energy after negating losses from optical design flaws such as tracking errors, condition and cleanliness of reflective mirrors and glazing. After this, the solar energy passes through the glass envelop ($q_{go,SAbs}$) and is absorbed by the receiver pipe ($q_{po,SAbs}$). The HTF receives

the energy after the energy absorbed by the receiver pipe is transferred via conduction from the outside of the pipe to the inside of the pipe ($q_{po-pi,cond}$) followed by convection from the inside of the pipe to the HTF ($q_{pi-htf,conv}$). Hence the following relationship can be established [36].

$$q_{pi-htf,conv} = q_{po-pi,cond} \tag{3.17}$$

Not all the energy is transferred to the HTF and is reflected back to the environment. A small portion of the energy that passes into the glass cover is reflected back to the glass envelope via convection ($q_{po-gi,conv}$) and radiation ($q_{po-gi,rad}$). This energy is then conducted through the glass cover wall via conduction ($q_{gi-go,cond}$). This energy and the energy absorbed by the glass cover wall is lost to the environment through convection ($q_{go-a,conv}$) and radiation ($q_{go-a,rad}$). Using these statements, the following equations can be formulated:

$$q_{po,SAbs} = q_{po-gi,conv} + q_{po-gi,rad} + q_{po-pi,cond} \tag{3.18}$$

$$q_{po-gi,conv} + q_{po-gi,rad} = q_{gi-go,cond} \tag{3.19}$$

$$q_{gi-go,cond} + q_{go,SAbs} = q_{go-a,conv} + q_{go-a,rad} \tag{3.20}$$

$$q_{Loss} = q_{go-a,conv} + q_{go-a,rad} \tag{3.21}$$

3.2.1.1 Heat Transfer between HTF and Receiver Pipe

From Newtons law of cooling, the following formulation of convective heat transfer and the heat transfer coefficient (h_f) can be applied between the inside of the receiver pipe and the HTF. All coefficients are formulated for per unit length of absorber piping.

$$q_{pi-htf,conv} = h_{htf}\pi D_{pi}\,(T_{pi} - T_{htf}) \tag{3.22}$$

$$h_{htf} = Nu_{Dpi}\frac{k_{htf}}{D_{pi}} \tag{3.23}$$

where Nu_{Dpi} is the Nusselt number for inside diameter of the receiver pipe. For turbulent flow (Re>2300), the following equation is used to calculate the Nusselt number:

$$Nu_{D_{pi}} = \frac{\frac{f_{pi}}{8\left(Re_{D_{pi}}-1000\right)Pr_{htf}}}{1+12.7\sqrt{f_{pi}/8\ (Pr_{htf}^{2/3}-1)}}\left(\frac{Pr_{htf}}{Pr_{pi}}\right)^{0.11} \quad (3.24)$$

where the Prandtl number Pr_{htf} is set as the HTF temperature T_{htf}, Pr_{pi} is the Prandtl number set at the inner side of the receiver pipe temperature T_{pi}. The Nusselt number is calculated for the following conditions:

$0.5<Pr_{htf}<2x10^3$ and $2300<Re_{D_{pi}}<5x\ 10^6$

$$f_{pi} = \left[1.82log(Re_{D_{pi}}) - 1.64\right]^{-2} \quad (3.25)$$

3.2.1.2 Heat Transfer within Receiver pipe

Using Fourier's law, the following equation can be used to evaluate the conduction heat transfer between the inner and outer wall of the receiver pipe per unit length of absorber tube:

$$q_{po-pi,cond} = \frac{2\pi k_p(T_{pi}-T_{po})}{\ln\left(\frac{D_{po}}{D_{pi}}\right)} \quad (3.26)$$

where the thermal conductivity of the pipe is defined as k_p at the mean temperature between the inner and outer wall of the pipe [36].

$$k_p = (0.013)T_{pi-po} + 15.2 \quad (3.27)$$

3.2.1.3 Heat transfer between glass cover and receiver pipe

The area between the glass cover and receiver pipe contains a vacuum and hence heat transfer occurs via molecular conduction instead of free convection [36].

$$q_{po-gi,conv} = \pi D_{po} h_{po-gi}(T_{po}-T_{gi}) \quad (3.28)$$

where the heat transfer coefficient between the glass cover and receiver pipe is defined as:

$$h_{po-gi} = \frac{k_{vac}}{\frac{D_{po}}{2In\left(\frac{D_{gi}}{D_{po}}\right)} + b\gamma\left(\frac{D_{po}}{D_{gi}}+1\right)} \quad (3.29)$$

where k_{vac} is the thermal conductivity within the vacuum (W/m°C) [37]:

$$b = \frac{(2-a)(9\gamma-5)}{2a(\gamma+1)} \tag{3.30}$$

$$\lambda = \frac{2.331\ x\ 10^{-20}(T_{po-gi}+273)}{P_a\delta^2} \tag{3.31}$$

where "δ" is the diameter of a molecule of air equaling to 3.55 x 10^{-10} m [37]. The heat transfer between the glass cover and receiver pipe via radiation can be expressed by the following equation [36]:

$$q_{po-gi,rad} = \frac{\sigma\pi D_{po}(T_{po}^4 - T_{gi}^4)}{\left(\frac{1}{\varepsilon_{po}} + \left(\frac{(1-\varepsilon_{gi})D_{po}}{\varepsilon_{gi}D_{gi}}\right)\right)} \tag{3.32}$$

3.2.1.4 Heat transfer to the environment from glass cover surface

Heat is dissipated to the environment via convection and radiation. The following equation is used to model the heat transfer to the environment via convection:

$$q_{go-a,conv} = h_{go-a}\pi D_{go}(T_{go} - T_a) \tag{3.33}$$

where $h_{go\text{-}a}$ is the convection heat transfer coefficient for air (W/m^2°C) and is evaluated by the following equation:

$$h_{go-a} = \frac{k_{air}}{D_{go}} Nu_{D_{go}} \tag{3.34}$$

k_{air} is the thermal conductivity of air and Nu_{Dgo} is the average Nusselt number for the outer diameter D_{go} for the glass cover. The Nusselt number can be calculated from the following equation:

$$\overline{Nu}_{D_{go}} = CRe_{D_{go}}^m Pr_a^n \left(\frac{Pr_a}{Pr_{go}}\right)^{\frac{1}{4}} \quad \left| \begin{array}{l} Where\ \ 0.7 < Pr_a < 500 \\ and\ 1 < Re_{Dgo} < 10^6 \end{array} \right. \tag{3.35}$$

where n = 0.36 for Prandtl numbers greater than 10 and n = 0.37 for Prandtl numbers less than equal to 10 respectively. C and m are set according the following Reynolds number conditions in Table 3.

Table 3: Constants for Eq (3.35) [37]

Re_{Dgo}	C	M
1-4x10^1	0.75	0.4
4x10^1- 1x10^3	0.51	0.5
1x10^3- 2x10^5	0.26	0.6
2x10^5 - 1x10^6	0.076	0.7

The heat transfer from the glass cover to the environment can be modelled using the following equation [36]

$$q_{go-s,rad} = (5.67 * 10^{-8})\, \varepsilon_{go} \pi D_{go} \left(T_{go}^4 - T_{sky}^4\right) \tag{3.36}$$

where ε_{go} is the coating emittance of the glass cover and is calculated as below (^{0}C) [36]

$$\varepsilon_{go} = 0.000327(T_{go} + 273.15) - 0.065971 \tag{3.37}$$

3.2.2 Optical efficiencies and parameters

The overall optical efficiency of the receiver pipe (η_{rec}) is a function of the optical efficiency of the glass envelop (η_g) and the emittance of the glass envelop (ε_{go}) [86] and is modeled as below:

$$\eta_{rec} = \eta_g \varepsilon_{go} \tag{3.38}$$

The optical efficiency of the glass envelop (η_g) is a function of the incident angle modifier (k_θ), which is a quadratic function of the solar incident angle "θ" and multiple optical efficiency parameters that are defined and stated below [36]

$$\eta_g = K_\theta e_{rsh} e_t e_{geo} e_{mird} e_{rd} e_{cl} \tag{3.39}$$

where:

$$k_\theta = cos(\theta) + 0.000884\theta - 0.00005369\theta^2 \text{[36]} \tag{3.40}$$

e_{rsh} = Receiver shadowing, assumed 0.960 [36]

e_t = Tracking error, assumed 0.994 [36]

e_{geo} = Geometry error (mirror alignment), 0.980 [36]

e_{mird} = Dirt on mirrors, assume 0.89 [36]

e_{rd} = Dirt on receiver, assume 0.955 [36]

e_{cl} = Clean mirror reflection, 0.99 [36]

The values for the efficiency parameters above are taken from experimental results from [86] to provide realistic results.

3.2.3 PTSC energy model and exergy model

Based on the heat transfer formulations and optical efficiency, the PTSC energy model can be modelled. The solar energy absorption by the receiver pipe can now be expressed in terms of the solar irradiance (q_{sol}), the optical efficiency of the glass envelope and the absorptivity of the receiver pipe (α_{env}).

$$q_{go,SAbs} = q_{sol}\eta_{env}\alpha_{env} \tag{3.41}$$

Finally, a heat removal factor is applied to find the useful solar energy that is transferred to the heat transfer fluid from the PTSC collector and can be defined as below [36]

$$F_R = \frac{\dot{m_{htf}}c_p}{A_r U_L}\left(1 - Exp\left[-\frac{U_L F' A_r}{\dot{m}c_p}\right]\right) \tag{3.42}$$

where F' is the PTSC collector efficiency factor and is defined as below:

$$F' = \frac{\frac{1}{U_L}}{\frac{1}{U_L} + \frac{D_{po}}{h_{htf}D_{pi}} + \left(\frac{D_{po}}{2k_{htf}} In\frac{D_{po}}{D_{pi}}\right)} \tag{3.43}$$

where U_L is the heat loss coefficient of the PTSC which is the sum of the coefficients for the heat transfer between all the PTSC components and with the environment due to conduction, convection and radiation.

Finally, the solar energy that is actually useful can be formulated by multiplying the heat removal factor with the solar energy absorbed by the receiver pipe:

$$\dot{Q}_{useful} = F_R \, q_{go,SAbs} \tag{3.44}$$

The PTSC is able to extract energy from the direct beam irradiation (G_{beam}); therefore the solar energy that is extracted by the collector can be defined by the equations below [39]:

$$\dot{Q}_{solar} = A_a \, . G_{beam} \tag{3.45}$$

where A_a is the aperture area of the collector.

Assuming all process are run at equilibrium and a steady state processes. The instantaneous thermal efficiency PTSC can be calculated by the equation below:

$$\eta_{th,collector} = \frac{\dot{Q}_{useful}}{\dot{Q}_{solar}} \tag{3.46}$$

The exergetic efficiency is calculated by finding the ratio between exergy of the heat transfer fluid within the receiver tube and the exergy flow from the solar radiation absorbed by the PTSC. Furthermore, the exergy destructed can be calculated from the exergy input and output.

$$\eta_{ex} = \frac{\dot{X}_{out,PTSC}}{\dot{X}_{in,PTSC}} \tag{3.47}$$

$$\dot{X}_{in,PTSC} = A_a G_{Beam} \left[1 + \frac{1}{3} \left(\frac{T_a}{T_{sun}} \right)^4 - \frac{4}{3} \left(\frac{T_a}{T_{sun}} \right) \right] \tag{3.48}$$

$$\dot{X}_{out,PTSC} = \dot{Q}_{useful} \left(1 - \frac{T_a}{T_{po}} \right) \tag{3.49}$$

$$\dot{X}_{out,PTSC} = \dot{X}_{des,PTSC} = \dot{X}_{in,PTSC} - \dot{X}_{out,PTSC} \tag{3.50}$$

3.2.4 PTSC input parameters

Using the formulated equations from sections 3.2.1 to 3.2.3, the PTSC model is generated. The input parameters to the system is provided in Table 4. The selection for the PTSC components, namely the solar collector, solar receiver and the heat transfer fluid is done in further sections based on parametric analysis completed on MATLAB software. The analysis is done using Abu Dhabi, UAE weather data as discussed in the literature review.

Table 4: PTSC Input Parameters

Parameter	Value
Solar Irradiance (W/m^2)	560
PTSC Solar Collector Selected	EuroTrough ET150
PTSC Solar Receiver Selected	Schott PTR70 2008
Selected HTF Fluid	Therminol VP-1
HTF Loop inlet Temperature (C)	293
HTF Loop outlet Temperature (C)	391
Total Apperature Area (m^2)	7006

3.3 Thermal Energy Storage

To provide energy to the system at hours with low and zero insolation from the sun, thermal energy storage system is added to the design. This increases the power output from the system and operating hours. Molten salts are stored in two containers in the TES system with a capacity of 8 hours for full load storage. One tank will be set as the "hot tank" and the other as "cold tank", where the hot tank is filled up during high insolation hours such that maximum molten salt will occupy in this tank. During low insolation hours, the molten salt is pumped from the hot tank to the cold tank after it transfers energy to the ORC fluid. The energy from the PTSC heating fluid is transferred directly to the molten salt via a heat exchanger. The following energy balance provides a model for the heat exchanger:

$$\dot{m}_{htf} C_{phtf} (T_o - T_i) = \dot{m}_{tes} C_{ptes} (T_{hot} - T_{cold}) \tag{3.51}$$

$T_{hot}\ and\ T_{cold}$ are the temperatures of the two tanks which store the molten salt presented in Tables 10 and 11. The capacity of the TES tanks are calculated, using software called SAM (Solar Advisor Model) which has data for molten salt (Hitec Salt,) and based on the power output requirement will calculate the required tank size, along with the input design parameters and the storage volume calculated on SAM (Solar Advisory Model).

3.4 Integrated Solar-Organic Rankine Cycle with TES model (ISORC)

The Integrated Solar Organic Rankine Cycle (ISORC) with TES contains three systems, the PTSC which collects the solar energy, the TES which stores this solar energy and the ORC which produces power using the solar energy extracted. When the PTSC collects enough energy to power the PTSC, the heating fluid within the PTSC directly transfers thermal energy to the Organic fluid which vaporizes in the heat exchanger. When the PTSC is collecting more than the required energy for power generation during high insolation hours, excess mass flow rate is transferred to the TES heat exchanger. The TES consists of two tanks, one containing cold molten salt and the other containing hot molten salt. The cold molten salt is pumped to the TES heat exchanger, where it is heated by the heating fluid from the PTSC and is then stored in energy demand from the ORC, the stored hot molten salt is pumped into the TES/ORC heat exchanger where the ORC fluid vaporizes and then goes to the ORC turbine for power generation,the hot salt tank. During low insolation hours, when the PTSC is not able to meet the while the hot molten salt loses thermal energy and is transferred to the cold salt tank. The salt is required to stay in a molten state with a minimum recommended temperature for Hitec molten salt at 142 ℃. Figure 11 shows the schematic of the ISORC with TES.

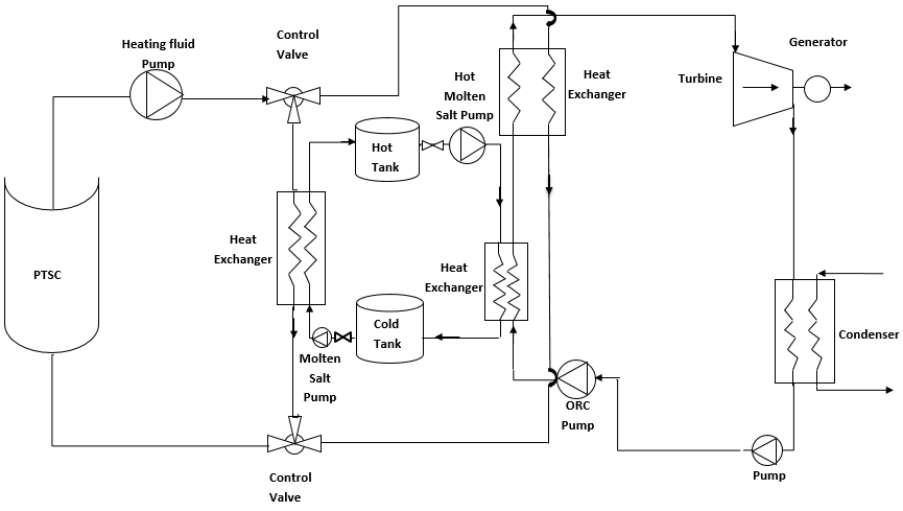

Figure 11: ISORC with TES schematic diagram

3.4.1 ISORC operation

The ISORC operation depends on the solar irradiation received by the system. The HTF mass flow rate varies during the day and due to this phenomenon, the system operation will vary. During high insolation hours, i.e. afternoon hours in Figure 13, when the mass flow rate of the HTF fluid exceeds the requirement to the ORC heat exchanger, fluid is directed to the PTSC/TES heat exchanger where the TES molten salt is heated and stored in the hot tank. During low insolation hours with the TES having no hot molten salt in the hot tank, i.e. morning hours in Figure 12, the HTF is supplied to the ORC in order to meet the energy demand.

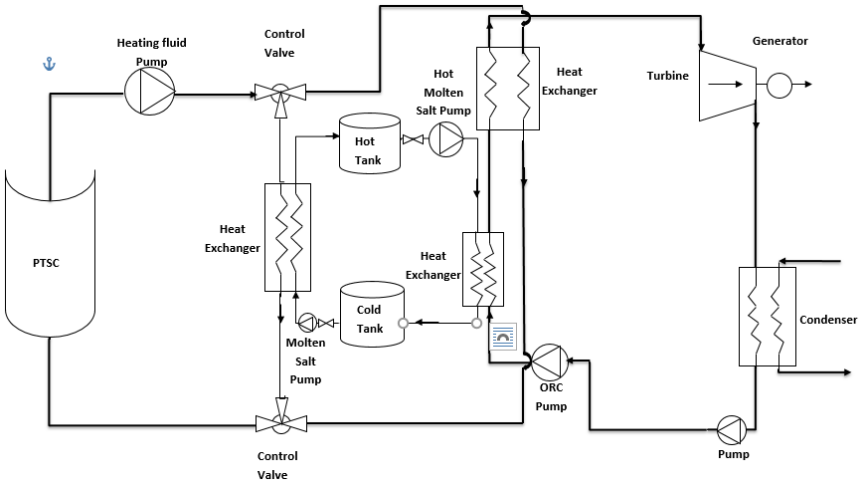

Figure 12: ISORC operation during morning hours (low solar insolation)

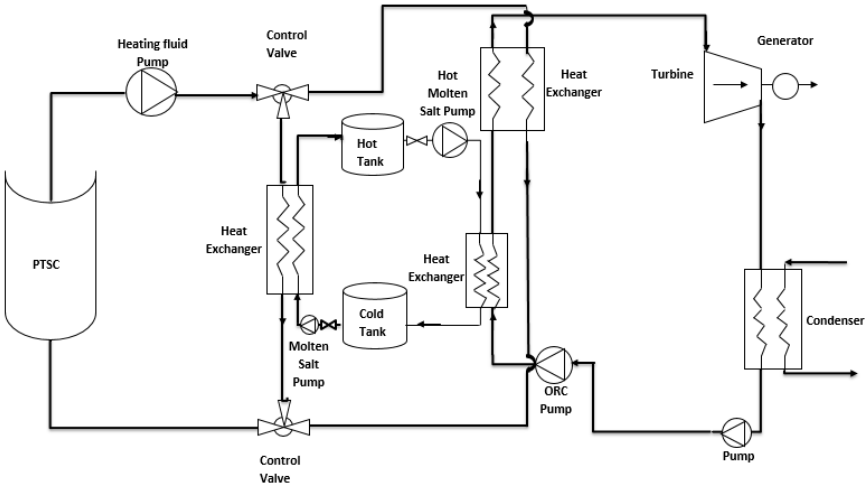

Figure 13: ISORC operation during afternoon hours (high solar insolation)

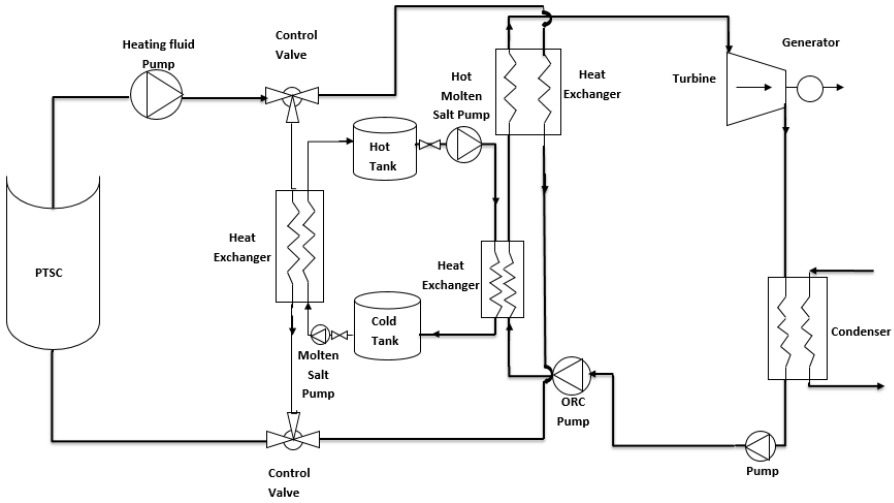

Figure 14: ISORC operation during evening hours (low solar insolation)

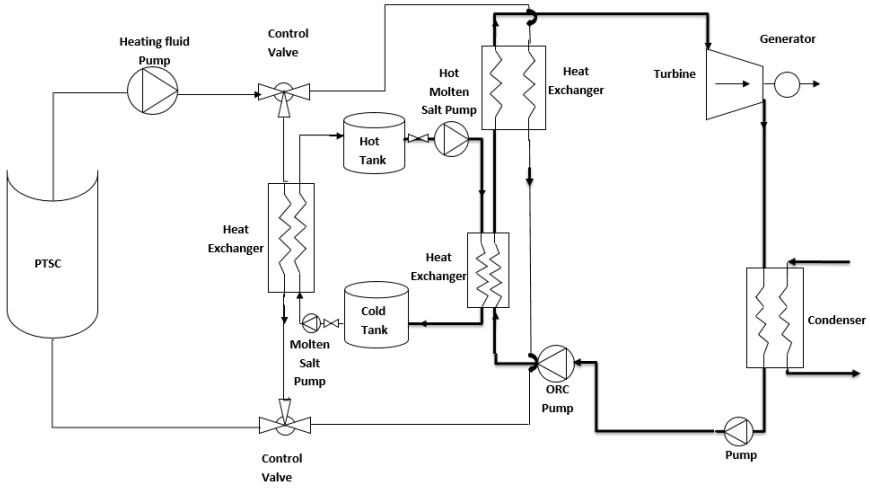

Figure 15: ISORC operation during night hours (zero solar insolation)

During this process, no HTF is supplied to the TES system. During hours where there is no solar irradiance, i.e. night hours in Figure 15, the hot molten salt from the TES hot tank is pumped out and heat is transferred to the ORC fluid for power output. The cold molten fluid is transferred to the cold tank. The HTF is not pumped during these hours. During low insolation with hot molten salt available in the hot tank, i.e. evening hours in Figure 14, when the HTF mass flow rate is not enough to provide the required power output from the ORC, ORC fluid is heated first from the hot molten salt, and then further heated by the HTF from the PTSC. These four cases explain the operation of the ISORC system integrated with TES for all possible conditions to be faced by the system.

3.5 Economic Model of the ISORC with TES

In this section, the cost of the system will be modelled with the objective of finding the levelized cost of electricity (LCOE) of the ISORC, the net capital cost and the net savings of the system. This will be done by setting cost equations to each component of the system. The aim is to evaluate if operating the system is feasible and comparable to the cost of electricity currently charged by DEWA. The savings made by operating the system is based on the LCOE difference between the ISORRC with 0, 5 and 8 hours of TES against the DEWA charge rate of electricity. It is to be noted that the installation cost for connected the grid to the rural location of our system is not considered in this calculation and therefore further savings is actually made by the ISORRC system.

3.5.1 Economic model for ORC

The equations for the components in these sections are obtained from SAM which will be run for different TES hours of operation. All cost equations are based on US dollars ($).

3.5.1.1 Turbine

The equation used to calculate the turbine capital cost is modelled as below used by SAM [65]:

$$Z_{orct} = 150(\dot{m}_{orc}w_{orct})\left(1 + e^{0.096(T_{T,inlet}-866)}\right)\left(\frac{50000}{\dot{m}_{orc}w_{orct}}\right)^{0.67} \tag{3.52}$$

3.5.1.2 Heat Exchangers

The capital cost of the heat exchangers used in the system can be modelled using the following equation [94]:

$$Z_{Hex} = 1.53 + 1.27\left(\frac{T_{h,inlet}}{623}\right)^{2.4} 10^{3.8528+0.4242\,ln\left(\frac{\dot{Q}_{Hex}}{0.018LMTD_{Hex}}\right)} \tag{3.53}$$

where

$\dot{Q}_{Hex}$ is the heat exchange rate (kW)

$LMTD_{Hex}$ is the log mean temperature difference (K)

$T_{h,inlet}$ is the hot fluid inlet temperature(K)

Cycle is also assumed to run as a heat exchanger; therefore equation (5.3) is used for the capital cost equation.

3.5.1.3 Pumps

The capital cost for pumps is modelled using the following equation [94]:

$$Z_p = 442\left[\dot{m}_{fluid} w_p\right]^{0.71} 1.41\left[1 + \left(\frac{0.2}{1-\eta_p}\right)\right] \tag{3.54}$$

Equation (5.4) is used for all the pumps in the system including for the PTSC, the molten salts and the ORC itself.

3.5.1.4 Condenser

The capital cost of the air-cooled condenser is as follow:

The capital investment cost of the steam condenser in $US\$$ is adapted from [94], and it is given by:

$$Z_c = 248\left(\frac{\dot{Q}_c}{2.2 LMTD_{cond}}\right) + 659\left(\frac{\dot{Q}_c}{48.1275}\right) \tag{3.55}$$

where

$\dot{Q}_c$ is the rate of heat transfer in the condenser (kW)

$LMTD_{cond}$ is the log mean temperature difference in the condenser (K)

3.5.2 PTSC field economic model

The capital cost of the PTSC system is shown modelled in equation 3.55 [70].

$$Z_{PTSC} = A_{solarfeild} C_{PTSC} + A_{solarfelid} C_{HTF} \tag{3.56}$$

where

$C_{PTSC}$is the PTSC cost constant and it equals $245\ \$/m^2$ [94]

$C_{TES}$is the TES cost constant and it equals $80\ \$/kWh$ [94]

$C_{HTF}$is the Heating Fluid cost constant and it equals $90\ \$/kWh$ [94]

3.5.3 Thermal energy storage economic model

The thermal energy storage capital cost is set as the following:

$$Z_{TES} = \dot{Q}_{tank} C_{TES} \tag{3.57}$$

where $\dot{Q}_{tank}$ is the thermal capacity of the TES storage tank.

3.5.4 Total installed cost

The total installed cost is modelled as the sum of the direct and indirect capital costs and the operational and maintenance cost from SAM with unit rates from [88]. The equations from the above sections are set and based on the weather data for Abu Dhabi, the system operation is analyzed and accordingly the cost model is applied and represented in Table 5.

Table 5: Total installed cost for ISORRC with 0, 5- and 8-hours operation of TES

Description	**Unit rate**	**Total Cost for ISORRC with TES 0hrs**	**Total Cost For ISORRC with TES 5hrs**	**Total Cost for ISORRC with TES 8hrs**
Solar Field	100 $/m^2	$ 1,962,000	$ 1,962,000	$ 1,962,000
HTF system	30 $/m^2	$ 588,600	$ 588,600	$ 588,600
TES Storage	45 $/kWht	$0	$ 632,022.50	$ 1,011,236
Power Plant	900 $/kWe	$ 900,000	$ 900,000	$ 900,000
Balance of Plant	90 $/kWe	$ 90,000	$ 90,000	$ 90,000
Site Improvements	5 $/m^2	$ 98,100	$ 98,100	$ 98,100
Contingency of total	3 % of subtotal	$ 109,161	$ 128,121	$513,896
Total Direct Cost		**$ 3,747,861**	**$ 4,398,844**	**$ 4,789,434**
EPC and Owner Cost	6% of Direct Cost	$ 224,871	$ 263,930	$ 287,366
Total land Cost	500 $/acre	$ 8,853	$ 8,853	$ 8,853
Total Indirect Cost		**$ 233,724**	**$ 272,783**	**$ 296,219**
Total Installed Cost		**$ 3,981,585**	**$ 4,671,627**	**$ 5,085,653**

The description for each of the direct and indirect costs from Table 5 are explained in the sections below.

3.5.4.1 Direct Capital Costs

A direct capital cost represents an expense for a specific piece of equipment or installation service that applies in year zero of the cash flow.

Site Improvements ($/m^2)

A cost per square meter of total reflective area.

PTSC Field ($/m^2)

A cost per square meter of total reflective area related to installation of the heliostats, including parts, field wiring, drives, labor, and equipment.

Balance of Plant ($/kWe)

A cost per electric kilowatt of power cycle gross capacity related to installation of the balance-of-plant components and controls, and construction of buildings, including labor and equipment.

Power Block ($/kWe)

A cost per electric kilowatt of power cycle gross capacity related to installation of the power block components, including labor and equipment.

Storage ($/kWht)

Cost per thermal megawatt-hour of storage capacity for the installation of a thermal energy storage system, including equipment and labor.

Contingency (%)

A percentage of the sum of the site improvements, PTSC field, balance of plant, power block, storage system costs to account for expected uncertainties in direct cost estimates.

Total Direct Cost ($)

The sum of improvements, site improvements, PTSC field, balance of plant, power block, storage system, and contingency costs.

3.5.4.2 Indirect Capital Costs

An indirect cost is typically one that cannot be identified with a specific piece of equipment or installation service.

Total Land Area

The total land area required for the project.

EPC and Owner Costs

EPC (engineer-procure-construct) and owner costs are associated with the design and construction of the project, permitting, royalty payments, consulting, management or legal fees, geotechnical and environmental surveys, interconnection costs, spare parts inventories, commissioning costs, and the owner's engineering and project development activities.

Total Land Costs

Costs associated with land purchases, which SAM calculates as the sum of non-fixed cost and fixed cost. Use the Land category described below for land costs, and inputs on the Financial Parameters page for financing costs.

Units for Land and EPC Costs

SAM calculates the total EPC and owner costs and total land costs by adding the four costs that can be specified using different units:

Cost per acre

A cost in dollars per total land area in acres.

% of Direct Cost

A cost as a percentage of total direct cost under direct capital cost.

Total Indirect Cost ($)

The sum of engineer-procure-construct costs, project-land-miscellaneous costs, and sales tax.

3.5.4.3 Total Installed Cost

The total installed cost is the sum of all the direct and indirect capital costs.

3.5.4.4 Operation and Maintenance Costs

Operation and Maintenance (O and M) costs represent annual expenditures on equipment and services that occur after the system is installed. Based on [87], Fixed annual cost and fixed cost by capacity are modelled on SAM to represent O and M costs.

Chapter 4. Results and Discussion

This chapter comprises of results and discussions from the system of equations and parameters that were defined in the previous chapter. The Organic Rankine Cycle (ORC) is optimized, and the organic fluid selection is done. The Regenerative Organic Rankine Cycle (RORC) is built and compared with the Organic Rankine Cycle. The Parabolic Trough Solar collector is modelled and analyzed. The heat transfer fluid is selected based on the heat transfer capabilities and mass flow rates. The solar collector and receiver are selected for the PTSC by comparative study using System Advisor Model (SAM). The Thermal Energy Storage System (TES) is designed based on RORC output using SAM software. Finally, the complete integrated system of the PTSC, RORC and TES is proposed with cost and comparison analysis.

4.1 Organic Rankine Cycle

The ORC is responsible for the power generation of the system. The most optimum ORC operating conditions are found in this section.

4.1.1 Organic fluid selection

A design output of 1MW is set from the system and configured as shown in Figure 5 in section 3.1. In order to select the optimum fluid for the system, fifteen fluids have been selected from the EES (Engineering Equation Solver) library, including refrigerants and various fluids. These fluids were categorized based on their critical pressures and critical temperatures. These fluids are shown in the Tables 6 to 8.

Table 6: Organic fluids with critical temperatures and pressures (Category A)

Organic Fluid	**Critical Temperature (°C)**	**Critical Pressure (kPa)**
R1234yf	94.7	3382
R134a	101	4059
R22	96.1	4989
R410a	71.3	4901

Table 7: Organic fluids with critical temperatures and pressures (Category B)

Organic Fluid	Critical Temperature (°C)	Critical Pressure (kPa)
Butene	146.1	4005
Isobutane	134.7	3640
Isopentane	187.2	3370
n-Butane	152	3796
R245fa	154	3651

Table 8: Organic fluids with critical temperatures and pressures (Category C)

Organic Fluid	Critical Temperature (°C)	Critical Pressure (kPa)
Benzene	288.9	4894
Cyclohexane	280.5	4081
Cyclopentane	238.6	4571
MDM	290.9	1415
n-Pentane	196.5	3364
Toluene	318.6	4126

Fifteen fluids have been categorized in order to better understand the result of running the respective ORC system. Since each fluid has its own characteristic critical temperature and pressure, the turbine inlet pressure condition is set to 80% of the critical pressure of the respective fluid to ensure that at no state within the cycle the fluid exceeds its critical temperature (subcritical ORC). Based on further set points listed below, the analysis is done for each fluid for their respective outcomes. Based on the

data and assumptions, the following results for exergy and energy analysis were found using EES in Tables 9 to 11.

From the results in Tables 9-11, it is observed that cyclopentane provides the highest energy efficiency while benzene provides the higher exergy efficiency. While the thermal efficiency of the ORC for most fluids is very similar for the results above, the mass flow rate for the cyclopentane fluid is the least, and therefore cyclopentane is selected as the ORC fluid. Furthermore, analysis with the independent ORC cycle and combined ORC with PTSC and TES systems are done using cyclopentane as the ORC fluid.

Table 9: Energy and exergetic efficiencies of ORC fluids (Category A)

Organic fluid	**Cycle efficiency**	**Mass flow rate (kg/s)**	**Exergy efficiency**
R1234yf	20.04%	19.59	18.27%
R134a	20.80%	16.93	18.68%
R22	20.48%	15.12	18.65%
R410a	20.54%	14.00	18.76%

Table 10: Energy and exergetic efficiencies of ORC fluids (Category B)

Organic fluid	**Cycle efficiency**	**Mass flow rate (kg/s)**	**Exergy efficiency**
Butene	20.37%	7.89	19.17%
Isobutane	20.47%	8.40	19.25%
Isopentane	18.91%	8.97	16.28%
n-Butane	21.02%	7.88	19.07%
R245fa	19.07%	18.02	17.55%

Table 11: Energy and exergetic efficiencies of ORC fluids (Category C)

Organic fluid	Cycle efficiency	Mass flow rate (kg/s)	Exergy efficiency
Benzene	21.37%	7.53	20.91%
Cyclohexane	18.45%	7.91	17.57%
Cyclopentane	21.50%	7.19	20.64%
MDM	8.452%	31.60	7.928%
n-Pentane	18.68%	8.82	16.01%
Toluene	18.55%	8.31	17.59%

4.1.2 Regenerative organic cycle vs simple organic Rankine cycle

A regenerative organic cycle is proposed in order to improve the ORC system. A regenerative organic cycle differs from the simple ORC, where an intermediate stream is bled from the turbine at an intermediary pressure point between the condenser pressure and the turbine inlet pressure. This stream is then used to increase the energy transferred to the ORC fluid entering the heat exchanger. Therefore, it reduces the load on the heat exchanger and improves the overall cycle efficiency. A systematic diagram for the regenerative organic Rankine cycle (RORC) is shown in Figure 16.

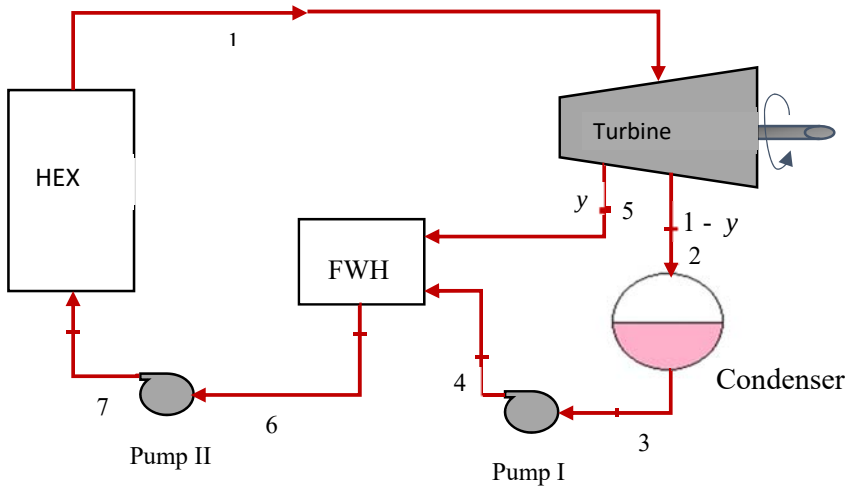

Figure 16: Regenerative organic rankine cycle schematic diagram

The turbine inlet pressure is set as 80% of the Cyclopentane critical pressure, and the condenser pressure is set to 10 kPa which are the same conditions as the ORC for comparison. A parametric analysis was carried out in EES to find the optimum pressure for the intermediate stream to be bled based on the cycle efficiency. The results are shown in Table 12 below.

Table 12: Comparison between ORC and RORC energy and exergetic efficiency

Cycle	Cycle Efficiency	Mass flow rate (kg/s)	Exergy Efficiency
Simple ORC	21.50%	7.191	20.64%
Regenerative ORC	22.42%	7.314	20.97%

An increase in cycle and exergy efficiencies is observed as well as an increase in the flow rate requirement of the system. Based on the obtained results, the Regenerative Organic Rankine Cycle will be implemented to the overall integrated system with the PTSC and TES. Parametric analysis is done on the RORC to further optimize the system. The effect of varying the intermediate pressure is observed against the cycle efficiency and exergy, and the following results are obtained and shown in Figures 17 and 18.

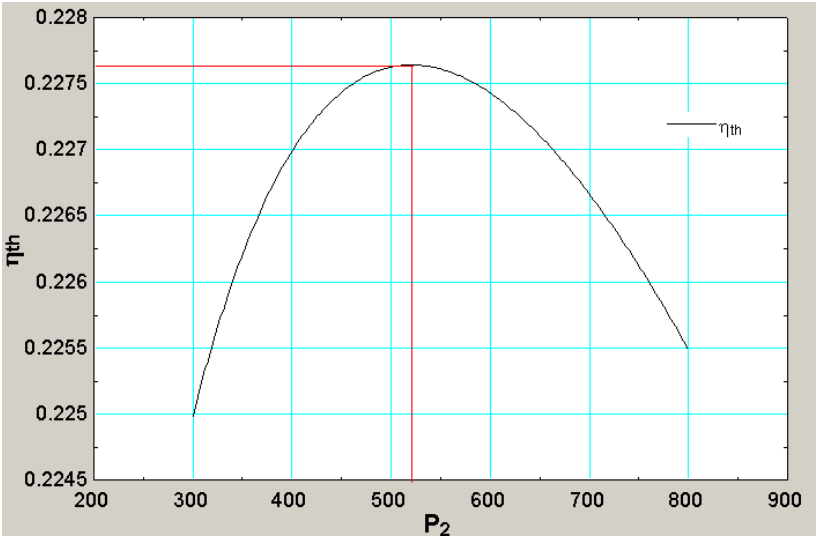

Figure 17: Intermediate pressure vs thermal efficiency of RORC

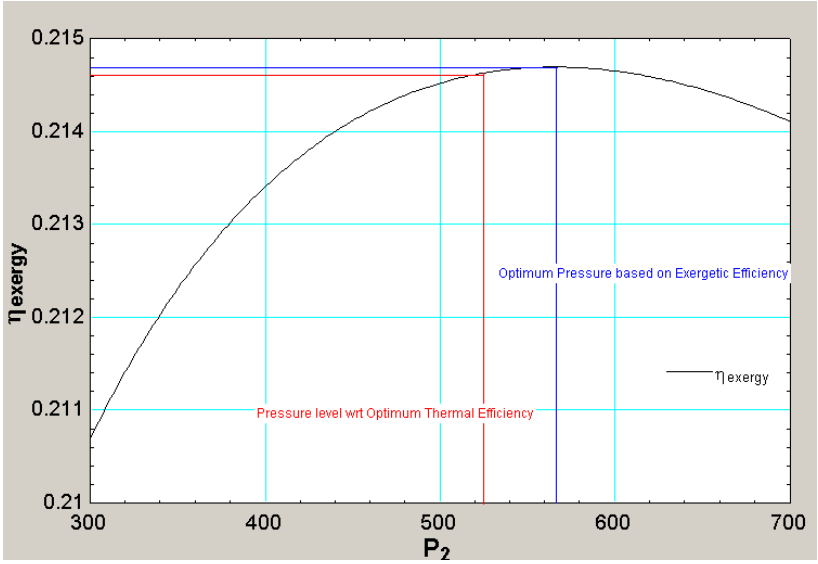

Figure 18: Effect of varying pressure on the exergetic efficiency of the RORC

Figure 17 shows that 525 kPa is the optimum intermediate pressure level to provide maximum efficiency from the cycle of 22.76%. Figure 18 shows that, at 565 kPa, maximum exergetic efficiency occurs, which is 21.47%. Furthermore, Figure 18 shows that at 525 kPa, 21.46% exergetic efficiency is obtained. Based on the findings, the intermediate pressure is fixed to 525 kPa for the complete integrated system of the RORC with the PTSC and TES systems.

4.1.3 Selected organic fluid vs water comparison

In order to further understand how Organic Rankine Cycles compare to standard Rankine cycles, the selected organic fluid, Cyclopentane, is compared with water for the same cycle output. However, unlike in the comparison where the fluids were all pressurized to 80% of their critical pressure at the turbine inlet, the Rankine cycle turbine inlet pressure will be set same as the pressure of the turbine inlet pressure of the Cyclopentane ORC. This is because 80% of the critical pressure of water is at 17.651 MPa, which is excessive and not required. The turbine inlet pressure is set to be at 3.657 MPa, which is 80% of the critical pressure of Cyclopentane, while all other cycle parameters remain the same as stated in section 4.1.2 in details. A comparison of the results from the two cycles is shown in Table 13.

Table 13: Conventional regenerative Rankine cycle vs RORC comparison

Description	Regenerative Rankine cycle (water)	RORC (Cyclopentane)
Specific heat capacity (kJ/kg K)	4.18	1.34
Critical pressure (MPa)	22.06	4.57
Critical temperature (C)	374	238.60
Mass flow rate of fluid (kg/s)	1.79	7.31
Cycle efficiency	34.24%	22.42%
Exergy efficiency	30.19%	20.97%
Thermal energy input required (kJ/kg)	2319.00	442.50
Specific net work output (kJ/kg)	794.10	99.21

From Table 13, it is seen how different the Cyclopentane and water operate to produce 1MW output from the power block. Water has a specific heat capacity almost 4 times that of Cyclopentane, meaning each kg of water can carry almost 4 times more energy as compared to Cyclopentane. Therefore, it is inevitable that the mass flow rate of water required for the output is less than compared to Cyclopentane, 1.799 kg/s for water as compared to 7.314 kg/s Cyclopentane. Furthermore, water shows better cycle efficiency and exergy as compared to Cyclopentane. An interesting factor is that much less thermal energy input is required per kg for Cyclopentane as compared to water, 442.5 kJ/kg to 2319 kJ/kg respectively which is almost 5 times more. This helps because the size of the PTSC and TES required becomes small. Multiplying the mass flow rate of fluids with their respective thermal energy input required, one can get the thermal power required for each cycle (3236.445kJ/s for Cyclopentane and 4171.881 kJ/s for water).

4.2 Parabolic Trough Solar Collector, Receiver and Heating Fluid Selection.

Three different fluids were selected for the PTSC system, Sylthem 800, Therminol VP-1 and Therminol 66. These fluids were compared based on the convective heat transfer coefficient, required pumping power and pressure drop per unit length of piping. Also the solar collector and Receiver is selected based on the thermal power output from the PTSC in this section.

4.2.1 Solar collector and receiver selection

The solar collector and receiver was selected based on doing a comparative study on SAM, where three solar collectors; EuroTrough ET150, Solargenix SGX-1 and SkyFuel Skytough and three solar receivers; Schott PTR70 2008, Schott PTR80 and Siemens UVAC 2010 were combined, and the best combination was selected, based on the monthly thermal power produced by the field. Tables 14 and 15 includes the technical data for the solar collectors and receivers.

Table 14: Solar collectors technical data

Solar Collector			
Parameter	**EuroTrough ET150**	**Solargenix SGX-1**	**SkyFuel SkyTrough**
Collector width (m)	5.75	5	6
Collector length (m)	12.5	8.33	14.375
Length of collector assembly (m)	150	100	115
Aperture Area (m2)	817.5	470.3	656
Tracking error	0.99	0.994	0.988
Optical efficiency	87.11%	87.46%	84.84%

For this comparative study, Therminol VP-1 was set as the fluid to provide 1MW output from the ORC with no TES provision, with results tabulated in Table 16.

Table 15: Solar receiver technical details

Solar Receiver			
Parameter	**Schott PTR70 2008**	**Schott PTR80**	**Siemens UVAC 2010**
Absorber tube inner diameter(mm)	66	76	60
Absorber tube outer diameter (mm)	70	80	14.375
Receiver efficiency	80%	82%	81.8%
Receiver Area (m2)	22	28	18
Receiver emissivity	0.92	0.93	0.92

Table 16: Thermal power produced from PTSC for three different solar collectors

Month	**Solargenix SGX-1**	**EuroTrough ET150**	**SkyFuel SkyTrough (with 80-mm OD receiver)**
Jan	856.65	1025.02	874.685
Feb	1036.36	1236.52	1049.01
Mar	1028.9	1232.46	1041.97
Apr	1187.7	1421.63	1206.14
May	1578.17	1881.19	1597.39
Jun	1572.83	1879.35	1597.25
Jul	1472.37	1767.68	1499.08
Aug	1502.5	1793.87	1523.27
Sept	1385.17	1652.55	1403.9
Oct	1272.83	1513.29	1286.66
Nov	949.504	1130.5	965.125
Dec	770.744	925.161	790.65
Total	**14613.728**	**17459.221**	**14835.13**

Table 16 shows that EuroTrough ET150 provides the largest amount of thermal power annually. Receivers are now compared, fixing EuroTrough ET150 as the solar collector to select the best receiver. Table 17 provides a comparison for the thermal

power produced from the field from three difference solar receivers fixing the solar collector as EuroTrough ET150

From Tables 16 and 17, it is observed that Schott PTR70 2008 receiver provides the best thermal power out, when combining with the EuroTrough ET150 collector. It is further also noticed how the thermal power produced by the field is maximum for the month of May for all combinations. While the month of December provides the lowest thermal power produced by the field. For further PTSC analysis, the solar collector and receiver are fixed as mentioned. Finally the technical specifications of the selected solar collector and receiver, the Schott PTR70 2008 receiver and EuroTrough ET150 collector, are displayed in Table 18. The absorber tube inner and outer diameters, the receiver efficiency, receiver area and receiver emissivity are tallied for Schott PTR70 2008 from SAM. Similarly the collector width, collector length, length of the assembly, number of modules and number of collectors, aperture area, tracking error and optical efficiency for the EuroTrough ET150 are displayed in Table 18.

Table 17: Comparison for thermal power produced from PTSC using three different solar receivers

Month	Schott PTR70 2008	Siemens UVAC 2010	Schott PTR80
Jan	1025.02	820.403	991.859
Feb	1236.52	868.292	1198.04
Mar	1232.46	838.385	1187.07
Apr	1421.63	939.348	1381.73
May	1881.19	1204.1	1832.58
Jun	1879.35	1190.62	1833.35
Jul	1767.68	1186.7	1719.05
Aug	1793.87	1177.98	1744.72
Sept	1652.55	1073.71	1607.65
Oct	1513.29	1068.14	1462.3
Nov	1130.5	872.991	1078.02
Dec	925.161	743.681	895.731
Total	**17459.221**	**11984.35**	**16932.1**

Table 18: Selected solar collector and receiver technical data

Receiver	
Parameter	Value
Type	Schott PTR70 2008
Absorber tube inner diameter(mm)	66
Absorber tube outer diameter (mm)	70
Receiver efficiency	80%
Receiver area (m2)	22
Receiver emissivity	0.92
Collector	
Type	EuroTrough ET150
Collector width (m)	5.75
Collector length (m)	12.5
Length of collector assembly (m)	150
Number of modulus	12
Number of collectors	1
Aperture area (m2)	817.5
Tracking error	0.99
Optical efficiency	87.11%

4.2.2 Heating fluid selection

Comparative study is done between the Therminol-VP1, Therminol 66 and Syltherm for the required convective heat transfer coefficient, pressure drop per unit length and pumping power of the fluids for different varying temperatures, using

equations from Chapter 3 on MATLAB software. Figures 19 to 21 show the results of the analysis.

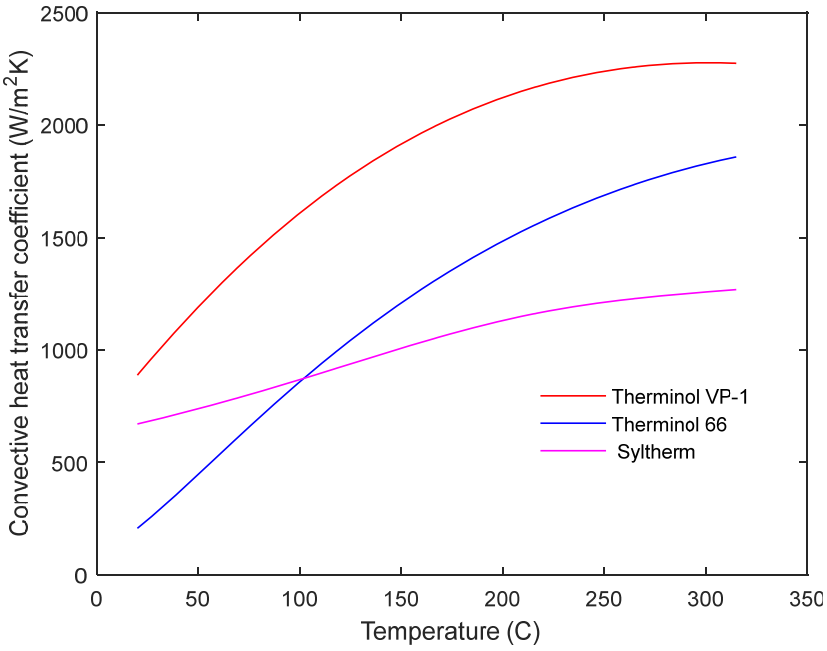

Figure 19: HTF convective heat transfer coefficient vs temperature

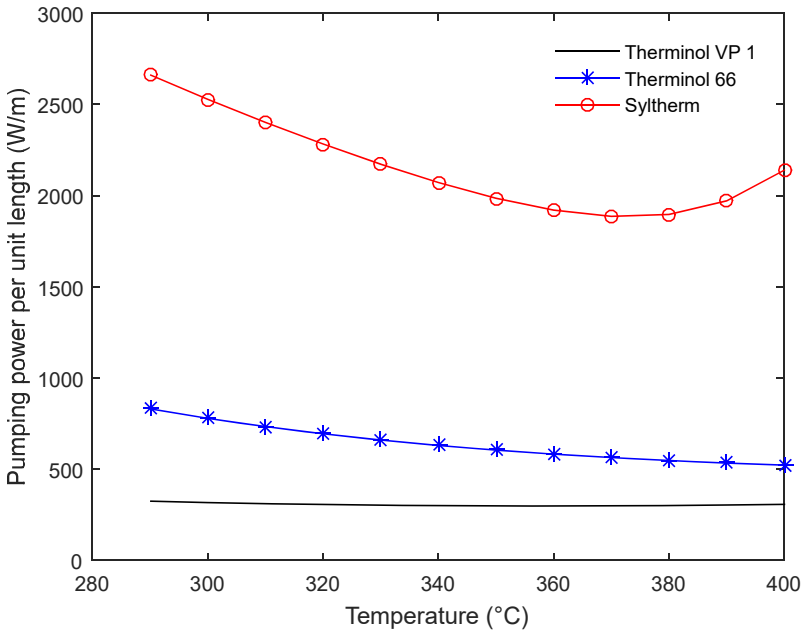

Figure 20: HTF pumping power per unit length vs temperature

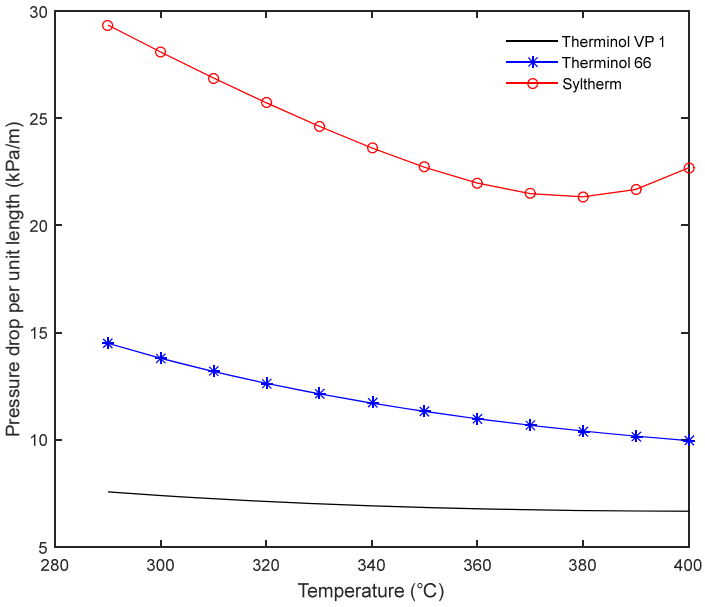

Figure 21: HTF pressure drop per unit length vs temperature

Figures 19 to 21 show that Therminol VP-1 requires the least pumping power per unit length and has the lowest pressure drop along the length of the pipe and the best convective heat transfer coefficient over all ranges of temperatures followed by Therminol 66 and Sytherm 88 respectively. Based on these findings, Therminol VP-1 is used as the heating fluid for the PTSC and design output shown from Figure 22-24.

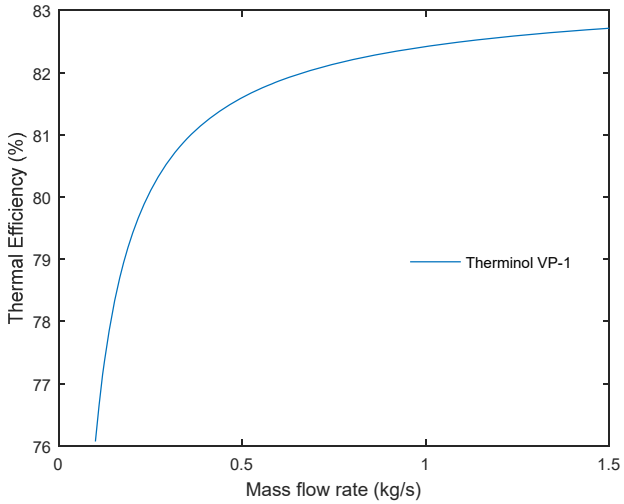

Figure 22: Thermal efficiency vs mass flow rate of Therminol VP-1

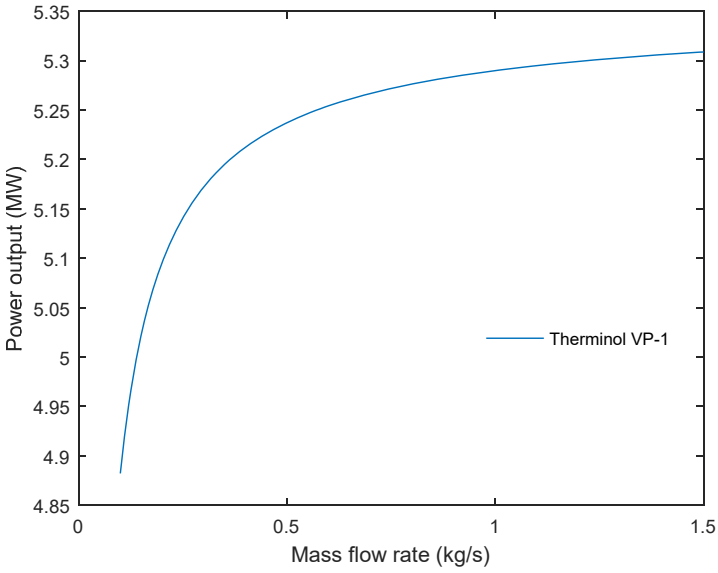

Figure 23: Power output from the PTSC system using Therminol VP-1

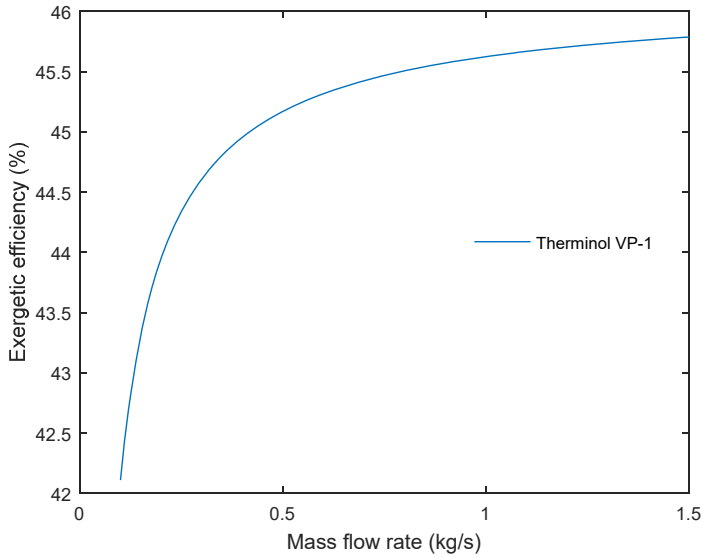

Figure 24: Exergetic efficiency vs mass flow rate of Therminol VP-1

From Figures 22 to 24, the PTSC thermal efficiency, exergetic efficiency and power out variation with mass flow rate of Therminol VP-1 can be observed. 1kg/s mass flow rate is set for our system as the design parameter, providing 82.4% thermal efficiency, 45.6% exergetic efficiency and 5.28MW power output from the system.

4.3 Thermal Energy Storage Material Selection

TES provides longer hours of operations of the system, and selecting the best material for the system is critical. A comparative study was done between three molten

salt materials: Hitec, Hitec Solar Salt and Hitec XL for system capacity. Table 19 shows results of the comparison for the required thermal capacity of 14.045 MW_{ht} for 5 hours of storage.

Table 19: Comparison between molten salts for TES material for 5 hours of storage

Material Description	**Hitec**	**Hitec XL**	**Hitec Solar Salt**
Storage Volume (m^3)	187.205	190.478	189.973
Specific Heat Capacity (kJ/kgK)	1.56	1.43294	1.50182
Density (kg/m^3)	1829.31	1957.3	1872.49

Hitec provides the lowest storage volume required to store the required thermal energy for the system, and is hence selected for our TES system. Hitec salt also has the highest specific heat capacity as compared to Hitec XL and Hitec Solar Salt. The specific heat capacity of molten salts is high and is utilized for the TES system. Technical data for the Hitec salt is given in Table 20 for 5 and 8 hours of TES operation.

Table 20: TES details with Hitec molten salt for 5 and 8 hours of operation

Parameter	**Symbol**	**Unit**	**Data for 5 hours TES**	**Data for 8 hours TES**
Storage Volume	V_{TES}	m^3	187.205	299.528
Tank Height	h_{tank}	m	20	20
Tank Diameter	D_{tank}	m	3.45222	4.36675
TES Thermal Capacity	$\dot{Q}_{tank}$	MWh	14.0449	22.4719
TES Capacity	$t_{storage}$	$hour$	5	8

Table 20 shows that the storage requirement for 8 hours is close to double ($299.528m^3$), as compared to storage operation of 5 hours ($187.205m^3$). Furthermore,

the thermal capacity required for 8 hours of TES operation increases to 22.4719 MWh, as compared to 14.0449 MWh thermal capacity required for 5 hours of TES operation.

4.4 Integrated Solar-Organic Regeneration Rankine Cycle with Thermal Energy Storage System (ISORRC with TES)

Based on the findings for the PTSC, TES and RORC system, the combined ISORRC system is then analyzed using SAM software for 0,5 and 8 hours of TES operation to evaluate the system outputs. The results are broken down for monthly and daily energy output results in order to understand the operations and outputs from the ISORRC system.

4.4.1 Monthly energy output

The monthly energy output for the ISORRC is determined using SAM software for 0, 5 and 8 hours of TES operation. Table 21 shows the results from SAM.

Table 21: Monthly energy from ISORRC with 0, 5 and 8 hours of TES operation

Month	0 Hours TES	5 Hours TES	8 Hours TES
Jan	145049	247172	300067
Feb	165562	265834	322533
Mar	159327	250101	300385
Apr	173321	258765	310344
May	223700	331799	401042
Jun	220872	324513	390832
Jul	221763	328889	393419
Aug	212791	318233	385666
Sep	197822	303129	367151
Oct	198957	308113	375385
Nov	170316	270002	326339
Dec	138759	229786	279513
Total	**2228239**	**3436336**	**4152676**

From Table 21, it is seen that May is the month where maximum energy is produced for all the system with 0,5 and 8 hours of TES operation and December is the month where minimum energy is produced from the ISORRC system for all three systems with 0, 5 and 8 hours of TES operation.

4.4.2 Daily energy output

Based on the monthly energy data, observation is made that maximum energy is produced during the month of May, while the minimum energy output from the system is observed during the month of December. To further understand the daily operation of the system in further detail, an average day is selected from May to simulate a "Sunny Day" where maximum power output is achieved by the system. An average day is selected from December to simulate a "Cloudy Day" where minimum power output is achieved by the system. This provides and insight on the best case scenario and worst case scenario of the operating conditions based on the varying weather conditions. The results are shown in Figures 25 to 27 for the ISORRC system with 0, 5 and 8 hours of TES operation.

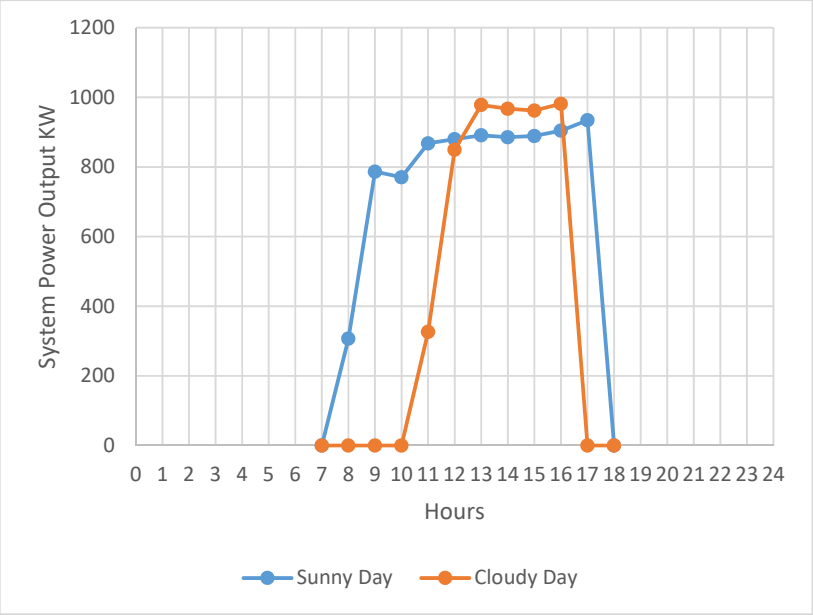

Figure 25: ISORRC power output for sunny and cloudy day with 0 hours TES

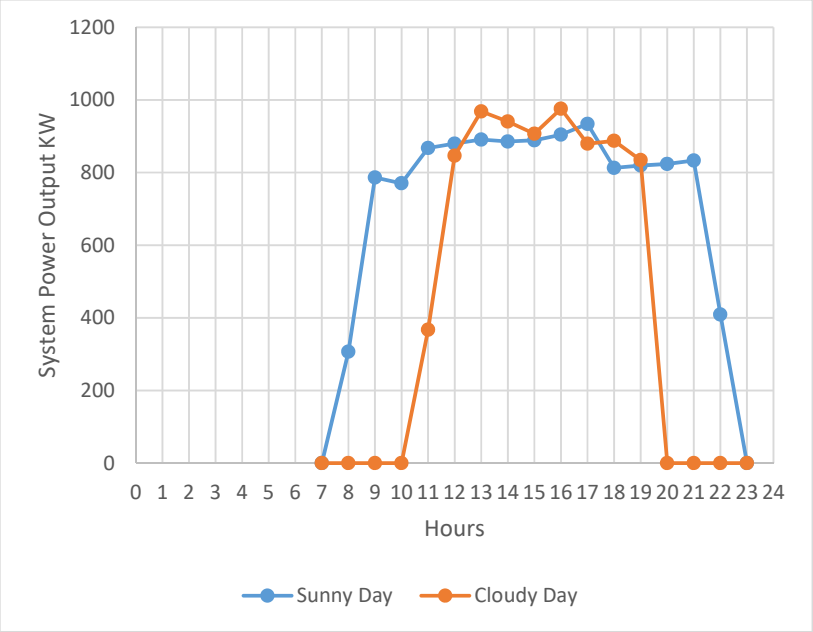

Figure 26: ISORRC power output for sunny and cloudy day with 5 hours TES

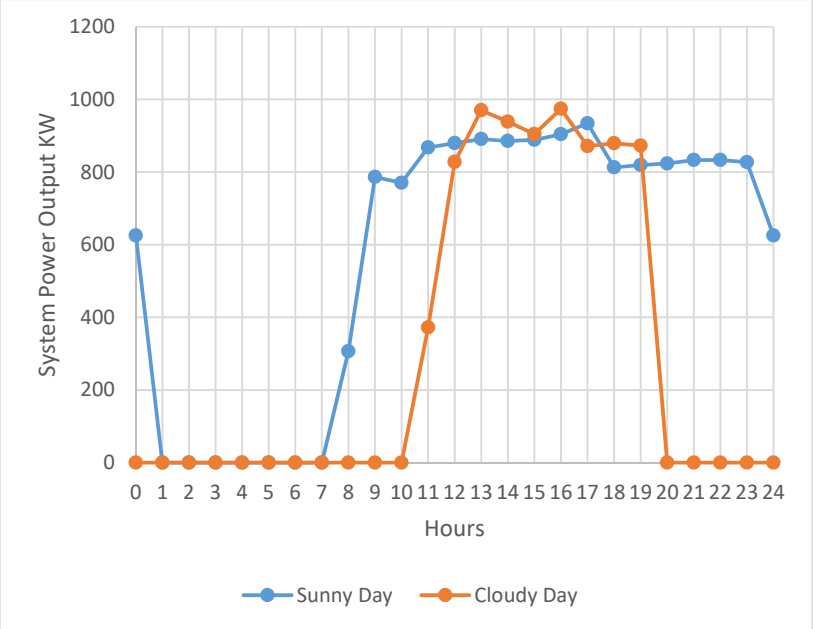

Figure 27: ISORRC power output for sunny and cloudy day with 8 hours TES

From Figures 25-27, interesting trends are observed. Figure 25 shows how the system will operate with no TES storage system for both sunny and cloudy days. For sunny days, the system would produce power output for 11 hours, whereas during cloudy days only 7 hours of power output is observed. An interesting finding is how on cloudy days the system produces a maximum power of over 950 KW, as compared to a sunny day where the maximum is closer 900KW. Comparing that with 5 hours of TES operation in Figure 26, the system provides power output for 17 hours for a sunny day, and 11 hours during cloudy days. This means that by adding TES of 5 hours, a cloudy day with TES would provide the same hours of power output from the system as it would for a sunny day from a system without TES.Finally, for 8 hours of TES operation from Figure 27, the system provides power output for 19 hours on a sunny day and 11 hours on a cloudy day. It can be seen that the difference of two hours of extra operation on a sunny day is observed between a TES system with 5 hours and 8 hours. Furthermore, the number of operating hours is the same on a cloudy day.

4.4.3 Annual results for the ISORRC with TES

Table 22 represents the annual costing, power consumption, energy produced results obtained from SAM. The CO_2 emission is calculated, using the model provided in [95]. Table 22, it is observed how adding a TES system to the ISORRC increases the overall cycle output and cycle efficiency and results in reduction in the LCOE. It can be observed that the LCOE for all three cases of 0, 5 and 8 hours of TES with the integrated is lower than the DEWA rate of electricity (38 fils/kWh as compared to 20, 15 and 13 files/kWh) which promotes the financial feasibility of operating the system. The annual energy output is almost doubled for 8 hours TES operation with the ISORRC, as compared to the ISORRC with 0 hours TES (from 2,228,239 kWh to 4,183,339kWh). Similarly, the LCOE is close to half for 8 hours of TES operation, as compared to 0 hours of TES. The same trend is observed in the carbon dioxide emissions that is saved by the ISORRC with TES. The maximum cycle efficiency varies only slightly from 39.44% to 39.55% for 0 hours of thermal energy storage to 8 hours of thermal energy storage. This indicates that the output from having increased operation hours is able to compensate for the losses by the integration of the TES to the integrated system. The plant life is designed for 35 years of operation. Savings by system is calculated based on the difference in LCOE between the DEWA rate and the

LCOE of the ISORRC. It should be noted that the savings by system per month does not include the cost of connection between conventional power plant to the location of the power plant, which includes grid connection, transformer costs and labor costs.

Table 22: ISORRC output for annual energy produced, LCOE and capital cost for TES operation of 0, 5 and 8 hours

Parameters	**ISORRC with 0 hours TES**	**ISORRC with 5 hours TES**	**ISORRC with 8 hours TES**
Annual Energy Produced (kWh)	2,228,239	3,433,416	4,183,339
Maximum Cycle Efficiency	39.44%	39.54%	39.55%
Plant Life (years)	35		
LCOE (¢/kWh)	5.43	4.08	3.59
LCOE (fils/kWh)	20	15	13
Average Monthly Load (kWh/month)	31,837.26		
DEWA electricity rate per month [96] (fils/kWh)	38		
Average DEWA electricity bill without system per month (AED)	12,098.15		
Savings by system per month (AED)	5,730.70	7,322.56	7,959.31
CO_2 emissions saved yearly by using ISORRC ($kgCO_2$)	403,497.10	628,006.30	757,533.27

Chapter 5. Conclusion and Recommendations

Initially, a study on the PTSC, ORC and TES system was done in order to obtain the best individual system and then integrate the optimum systems together with an analysis of the ISORRC with TES system. A study was done on various organic fluids which were categorized based on their critical pressures and temperatures. Based on the energy and exergetic efficiencies, the best ORC fluid was selected. A RORC was proposed, and an improvement in efficiency was observed. The heating fluid in the PTSC was selected based on the outcomes for convective heat transfer coefficients and their pumping power requirement per unit length. The molten salt was selected for the TES system, and a comparative study was done between several salts to provide the best solution for the system. Finally, the integrated system was analyzed based on yearly, monthly and daily parameters. The cost of the combined system and further financial parameters were reported. In this chapter, the conclusion and recommendations are discussed.

5.1 Conclusion

Fifteen fluids were analyzed for the ORC. Cyclopentane provided the best thermal and exergetic efficiency out of the fifteen fluids for the ORC system. The ORC system was analyzed on EES, and cyclopentane provided a thermal and exergetic efficiency of 21.50% and 20.64% respectively for a mass flow rate of 7.191 kg/s. Cyclopentane provided the respective thermal and exergetic efficiencies for a lower mass flow rates, as compared to other ORC fluids. An RORC was then proposed, where a feed water heater was added to an intermediary pressure line between the turbine inlet and condenser pressure. From parametric analysis done on EES software, it was found that the feed water heater should operate at 525 kPa to provide thermal and exergetic efficiency of 22.76% and 21.46%, which is higher than the ORC system efficiencies.

To optimize the PTSC system, the solar collector and receiver had to be selected. For a fixed heating fluid (Therminol VP-1) and fixed required output from the system (1 MWe), three different solar collectors and solar receivers were combined, and the monthly thermal power from the PTSC was observed. The analysis was done on SAM software. It was found that the Schott PTR70 2008 receiver and EuroTrough ET150 collector were the best combination to provide maximum power to the power

block. Once the solar collector and receiver were selected, parametric analysis was done on selecting the best heating fluid. Based on convective heat transfer coefficients, pumping power per unit length, thermal and exergetic efficiency, it was found that Therminol VP-1 provided most favorable as compared to Therminol 66 and Syltherm 88.

The TES system has two storage tanks, in which molten salts were stored in two tanks, one hot tank and one cold tank. Three molten salts were considered Hitec, Hitec XL and Hitec Solar salts. For a thermal storage capacity for 5 hours of operation, it was found that Hitec required the least storage space, and was therefore selected for our system.

Finally, the ISORRC with TES for 0, 5 and 8 hours of operation was analyzed on SAM for LCOE, and cost savings and annual energy was produced. As expected, by adding the TES system, an increase in annual energy output was observed resulting in a doubling from 2,228,239 kWh to 4,183,339 kWh for system with 0 hours TES and 8 hours TES respectively. This increase in output is seen with an increase in capital investment by 21.70% between the two systems from $ 3,981,586 to $ 5,085,653. Furthermore, the LCOE decreases from 5.43 ¢/kWh to 3.59 ¢/kWh between the ISORRC with 0 hours TES and 8 hours TES respectively. All these outcomes prove that a higher initial investment would provide increased hours of operation for the system and higher return to the system. All three systems had a lower LCOE rate, as compared to DEWA electricity rate of 38 fils per kWh and therefore gave further backing to the system. When comparing the ISORRC with 5 hours and 8 hours of TES, it was found, as expected, that the capital cost increases from $ 4,671,627 to $ 5,085,653 respectively. This was a 8.14% increase in capital investment, resulting in the annual energy produced to increase from 3,433,416 kWh to 4,183,339 kWh for ISORRC with 5 hours and 8 hours of TES respectively, which was an increase by 17.92%.

Simulation for a sunny day is done by selecting an average day in May, which provides the highest power output from the ISORRC. Furthermore, a cloudy day from an average day in December provided the lowest output from the ISORRC. The hourly data for all three systems was observed for all three ISORRC systems with 0,5 and 8 hours of TES operation. As expected, the hours of operation for the systems with TES was higher, compared to the system without TES and particularly during cloudy days;

the ISORRC with 0 hours of TES could only operate for 7 hours as compared to 10 hours of operation for both ISORRC with 5 and 8 hours of TES. It was found that although annually the 8 hour TES system provided higher power output, during a cloudy day, both system operated for the same number of hours. The ISORRC system with 8 hours of TES particularly provided energy to take the system load for 18 hours. This was particularly appealing since during summer weather in UAE, the electricity load is higher due to air-conditioning loads and other factors.

Overall, it can be concluded that the system proposed in this thesis provides a water free system that can operate in Dry-Humid conditions (UAE) and provide 1MW power output for 18 hours in a day for most optimal conditions. It must be noted that though capital costs are high, and the ROI for the system is over 200 years, which is not feasible. But since the system is of a small-medium scale, it is considered a worth making investment. The knowledge and the steps taken towards clean energy are necessary to move forward. This system will provide clean energy for a community where it is expensive to provide high tension cabling as it is geographically not accessible to power sources. Governments and NGO's should look into investing on such projects in countries and locations where electricity is not available. This system also has logical usage for locations where there is scarcity of water.

5.2 Recommendations

It is recommended to analyze with other ORC fluids that have not been considered in this study in order to improve the overall efficiency of the system. Further ORC cycle improvements can be done. Adding a recuperator to the ORC to utilize the turbine exit thermal energy and heating the inlet stream to the heat exchanger hence may improve the overall efficiency of the ISORRC system by reducing the load on the PTSC and TES systems.

Using different materials for the thermal energy storage system is recommended in order to reduce the cost of the system. This could be done by using the heating fluid as the storage fluid. This will reduce the number of heat exchangers needed in the system. A study in phase change materials that can be used as TES fluid can also be done to find an even more feasible solution.

The overall cost of the ISORRC system is high with relatively low net savings achieved by the system, which results in a long payback period. This is largely the reason why a small system for an Organic Rankine Cycle is proposed. The main reason is that organic fluids have smaller heat compared to water, and a larger mass flow rate is required to carry the same energy as water.

Although the solar insolation cannot be controlled, further study into improving the system output during cloudy days needs to be looked into. Alternative sources of energy during low solar insolation days should be considered in order to meet the power demand.

Finally, this system can be analyzed for underdeveloped countries and areas where electricity is still not accessible, and with low resources of water, as the proposed system does not require water for operational purpose, although cleaning the PTSC glass receiver/collectors is necessary.

References

[1] "Online data and tools for solar energy projects." Internet: http://solargis.info/ 2015, Jan. 1, 2015 [Jun. 20, 2016].

[2] G. Xu, G. Song, X. Zhu, W. Gao, H. Li and Y. Quan, "Performance evaluation of a direct vapor generation supercritical ORC system driven by linear Fresnel reflector solar concentrator," *Applied Thermal Engineering*, vol. 80, pp. 196-204, 2015.

[3] M. Marion, I. Voicu and A. Tiffonnet, "Study and optimization of a solar subcritical organic Rankine cycle," *Renewable Energy*, vol. 48, pp. 100-109, 2012.

[4] Cheng Zhou, "Hybridisation of solar and geothermal energy in both subcritical and supercritical Organic Rankine Cycles," *Energy Conversion and Management*, vol. 81, pp. 72-82, 2014.

[5] S. Quoilin, M. Broek, S. Declaye, P. Dewallef and V. Lemort, "Techno-economic survey of Organic Rankine Cycle (ORC) systems," *Renewable and Sustainable Energy Reviews*, vol. 22, pp. 168-186, 2013.

[6] Y. Feng, Y. Zhang, B. Li, J. Yang and Y. Shi, "Comparison between regenerative organic Rankine cycle (RORC) and basic organic Rankine cycle (BORC) based on thermoeconomic multi-objective optimization considering exergy efficiency and levelized energy cost (LEC)," *Energy Conversion and Management*, vol. 96, pp. 58-71, 2015.

[7] A. Meroni, J. Andreasen, G. Persico and F. Haglind, "Optimization of organic Rankine cycle power systems considering multistage axial turbine design," *Applied Energy*, vol. 209, pp. 339-354, 2018.

[8] H. Zhai, Q. An and L. Shi, "Zeotropic mixture active design method for organic Rankine cycle," *Applied Thermal Engineering*, vol. 129, pp. 1171-1180, 2018.

[9] S. Katulić, M. Čehil and D. Schneider, "Thermodynamic efficiency improvement of combined cycle power plant's bottom cycle based on organic working fluids," *Energy*, vol. 147, pp. 36-50, 2018.

[10] G. Györke, U. Deiters, A. Groniewsky, I. Lassu and A. Imre, "Novel classification of pure working fluids for Organic Rankine Cycle," *Energy*, vol. 145, pp. 288-300, 2018.

[11] M. Lukawski, R. DiPippo and J. Tester, "Molecular property methods for assessing efficiency of organic Rankine cycles," *Energy*, vol. 142, pp. 108-120, 2018.

[12] C. Noriega Sanchez, L. Gosselin and A. K. da Silva, "Designed binary mixtures for subcritical organic Rankine cycles based on multiobjective optimization," *Energy Conversion and Management*, vol. 156, pp. 585-596, 2018.

[13] B. Dong, G. Xu, T. Li, Y. Quan and J. Wen, "Thermodynamic and economic analysis of zeotropic mixtures as working fluids in low temperature organic Rankine cycles," *Applied Thermal Engineering*, vol. 132, pp. 545-553, 2018.

[14] E. Bellos and C. Tzivanidis, "Investigation of a hybrid ORC driven by waste heat and solar energy," *Energy Conversion and Management*, vol. 156, pp. 427-439, 2018.

[15] E. Saloux, M. Sorin, H. Nesreddine and A. Teyssedou, "Reconstruction procedure of the thermodynamic cycle of organic Rankine cycles (ORC) and

selection of the most appropriate working fluid," *Applied Thermal Engineering*, vol. 129, pp. 628-635, 2018.

[16] Y. Ding, C. Liu, C. Zhang, X. Xu, Q. Li and L. Mao, "Exergoenvironmental model of Organic Rankine Cycle system including the manufacture and leakage of working fluid," *Energy*, vol. 145, pp. 52-64, 2018.

[17] F. Yang, H. Cho, H. Zhang, J. Zhang and Y. Wu, "Artificial neural network (ANN) based prediction and optimization of an organic Rankine cycle (ORC) for diesel engine waste heat recovery," *Energy Conversion and Management*, vol. 164, pp. 15-26, 2018.

[18] K. Braimakis and S. Karellas, "Exergetic optimization of double stage Organic Rankine Cycle (ORC)", *Energy*, vol. 149, pp. 296-313, 2018.

[19] L. Li, Y. Ge, X. Luo and S. Tassou, "Design and dynamic investigation of low-grade power generation systems with CO_2 transcritical power cycles and R245fa organic Rankine cycles," *Thermal Science and Engineering Progress*, vol. 8, pp. 211-222, 2018.

[20] M. White, O. Oyewunmi, M. Chatzopoulou, A. Pantaleo, A. Haslam and C. Markides, "Computer-aided working-fluid design, thermodynamic optimisation and thermoeconomic assessment of ORC systems for waste-heat recovery," *Energy*, vol. 161, pp. 1181-1198, 2018.

[21] A. Habibollahzade, E. Gholamian, P. Ahmadi and A. Behzadi, "Multi-criteria optimization of an integrated energy system with thermoelectric generator, parabolic trough solar collector and electrolysis for hydrogen production," *International Journal of Hydrogen Energy*, vol. 43, no. 31, pp. 14140-14157, 2018.

[22] A. Mahmoudi, M. Fazli and M. Morad, "A recent review of waste heat recovery by Organic Rankine Cycle," *Applied Thermal Engineering*, vol. 143, pp. 660-675, 2018.

[23] H. Nami, A. Nemati and F. Jabbari Fard, "Conventional and advanced exergy analyses of a geothermal driven dual fluid organic Rankine cycle (ORC)," *Applied Thermal Engineering*, vol. 122, pp. 59-70, 2017.

[24] S. Seyedkavoosi, S. Javan and K. Kota, "Exergy-based optimization of an organic Rankine cycle (ORC) for waste heat recovery from an internal combustion engine (ICE)," *Applied Thermal Engineering*, vol. 126, pp. 447-457, 2017.

[25] M. Ebrahimi and K. Ahookhosh, "Integrated energy–exergy optimization of a novel micro-CCHP cycle based on MGT–ORC and steam ejector refrigerator," *Applied Thermal Engineering*, vol. 102, pp. 1206-1218, 2016.

[26] A. Benato, A. Stoppato, A. Mirandola and M. Del Medico, "Design and Off-Design Analysis of an ORC Coupled with a Micro-Gas Turbine," *Energy Procedia*, vol. 129, pp. 551-558, 2017.

[27] F. Aziz, R. Mudasar and M. Kim, "Exergetic and heat load optimization of high temperature organic Rankine cycle," *Energy Conversion and Management*, vol. 171, pp. 48-58, 2018.

[28] P. Morrone, A. Algieri, T. Castiglione, D. Perrone and S. Bova, "Investigation of Integrated Organic Rankine Cycles and Wind Turbines for Micro-Scale Applications," *Energy Procedia*, vol. 148, pp. 986-993, 2018.

[29] Z. Mat Nawi, S. Kamarudin, S. Sheikh Abdullah and S. Lam, "The potential of exhaust waste heat recovery (WHR) from marine diesel engines via organic Rankine cycle," *Energy*, vol. 166, pp. 17-31, 2018.

[30] X. Wang, G. Shu, H. Tian, W. Feng, P. Liu and X. Li, "Effect factors of part-load performance for various Organic Rankine cycles using in engine waste heat recovery," *Energy Conversion and Management*, vol. 174, pp. 504-515, 2018.

[31] S. Anvari, H. Taghavifar and A. Parvishi, "Thermo- economical consideration of Regenerative organic Rankine cycle coupling with the absorption chiller systems incorporated in the trigeneration system," *Energy Conversion and Management*, vol. 148, pp. 317-329, 2017.

[32] J. Li, G. Gao, G. Pei, P. Li, Y. Su, J. Ji and S. Riffat, "A novel concentrated solar power system using cascade steam-organic Rankine cycle and two-stage accumulators," *Energy Procedia*, vol. 142, pp. 386-394, 2017.

[33] G. Esquivel Patiño and F. Nápoles Rivera, "Global warming potential and net power output analysis of natural gas combined cycle power plants coupled with CO_2 capture systems and organic Rankine cycles," *Journal of Cleaner Production*, vol. 208, pp. 11-18, 2018.

[34] H. Helvaci and Z. Khan, "Thermodynamic modelling and analysis of a solar organic Rankine cycle employing thermofluids," *Energy Conversion and Management*, vol. 138, pp. 493-510, 2017.

[35] Y. Yang, H. Zhang, Y. Xu, F. Yang, Y. Wu and B. Lei, "Matching and operating characteristics of working fluid pumps with organic Rankine cycle system," *Applied Thermal Engineering*, vol. 142, pp. 622-631, 2018.

[36] İ. Yılmaz and A. Mwesigye, "Modeling, simulation and performance analysis of parabolic trough solar collectors: A comprehensive review," *Applied Energy*, vol. 225, pp. 135-174, 2018.

[37] G. O'Keeffe, S. Mitchell, T. Myers and V. Cregan, "Modelling the efficiency of a nanofluid-based direct absorption parabolic trough solar collector," *Solar Energy*, vol. 159, pp. 44-54, 2018.

[38] A.Mwesigye, İ. Yılmaz and J. Meyer, "Numerical analysis of the thermal and thermodynamic performance of a parabolic trough solar collector using SWCNTs-Therminol VP-1 nanofluid," *Renewable Energy*, vol. 119, pp. 844-862, 2018.

[39] M. Marefati, M. Mehrpooya and M. Shafii, "Optical and thermal analysis of a parabolic trough solar collector for production of thermal energy in different climates in Iran with comparison between the conventional nanofluids," *Journal of Cleaner Production,* vol. 175, pp. 294-313, 2018.

[40] F. Bioucas, S. Vieira, M. Lourenço, F. Santos, and C. Nieto de Castro, "Performance of heat transfer fluids with nanographene in a pilot solar collector." *Solar Energy*, 172, pp.171-176, 2018.

[41] H. Singh and R. Mishra, "Performance analysis of solar parabolic trough collectors driven combined supercritical CO 2 and organic Rankine cycle," *Engineering Science and Technology, an International Journal*, vol. 21, no. 3, pp. 451-464, 2018.

[42] A. Abdulhamed, N. Adam, M. Ab-Kadir and A. Hairuddin, "Review of solar parabolic-trough collector geometrical and thermal analyses, performance, and applications," *Renewable and Sustainable Energy Reviews*, vol. 91, pp. 822-831, 2018.

[43] H. Bhowmik and R. Amin, "Efficiency improvement of flat plate solar collector using reflector," *Energy Reports*, vol. 3, pp. 119-123, 2017.

[44] D. Eryener, J. Hollick and H. Kuscu, "Thermal performance of a transpired solar collector updraft tower," *Energy Conversion and Management*, vol. 142, pp. 286-295, 2017.
[45] Q. Zou, Z. Li and H. Wu, "Modal analysis of trough solar collector," *Solar Energy*, vol. 141, pp. 81-90, 2017.
[46] H. Hoseinzadeh, A. Kasaeian and M. Behshad Shafii, "Geometric optimization of parabolic trough solar collector based on the local concentration ratio using the Monte Carlo method," *Energy Conversion and Management*, vol. 175, pp. 278-287, 2018.
[47] L. Xu, F. Sun, L. Ma, X. Li, G. Yuan, D. Lei, H. Zhu, Q. Zhang, E. Xu and Z. Wang, "Analysis of the influence of heat loss factors on the overall performance of utility-scale parabolic trough solar collectors," *Energy*, vol. 162, pp. 1077-1091, 2018.
[48] C. Arun and P. Sreekumar, "Modeling and performance evaluation of parabolic trough solar collector desalination system," *Materials Today: Proceedings*, vol. 5, no. 1, pp. 780-788, 2018.
[49] S. Marrakchi, Z. Leemrani, H. Asselman, A. Aoukili and A. Asselman, "Temperature distribution analysis of parabolic trough solar collector using CFD," *Procedia Manufacturing*, vol. 22, pp. 773-779, 2018.
[50] E. Batuecas, C. Mayo, R. Díaz and F. Pérez, "Life Cycle Assessment of heat transfer fluids in parabolic trough concentrating solar power technology," *Solar Energy Materials and Solar Cells*, vol. 171, pp. 91-97, 2017.
[51] S. Heidsieck, S. Dörrich, R. Weidner and B. Rieger, "Branched siloxanes as possible new heat transfer fluids for application in parabolic through solar thermal power plants," *Solar Energy Materials and Solar Cells*, vol. 161, pp. 278-284, 2017.
[52] N.S. Suresh, N.C. Thirumala, B.S. Rao and M.A. Ramaswamy, "Methedology of sizing the solar field for parabolic trough technology with thermal storage and hybridization," S*olar Energy*, vol. 110, pp. 247-259, 2014.
[53] V. Poghosyan and M.I. Hassan, "Techno-economic assessment of substituting natural gas based heater with thermal energy storage system in parabolic trough concentrated solar power plant," *Renewable Energy*, vol. 75, pp. 152-164, 2015.
[54] Y. Li, N. Zhang, "Performance comparison of two low-CO_2 emission solar/methanol hybrid combined cycle power systems," *Applied Energy*, vol. 155, pp 740-752, 2015.
[55] S. Acharya, S. Bhattacharjee, "Analysis and characterization of wind-solar-constant torque spring hybridized model," *Energy*, vol. 8, no. 3, pp. 279-289, 2014.
[56] S. Peng, H. Hong and H. Jin, "Triple cycle for solar thermal power system adapted to periods with varying insolation," *Energy*, vol 60, pp. 129-138, 2013.
[57] H. Athari, S. Soltani, S. Mahmoudi, M. Rosen and T. Morosuk, "Exergoeconomic analysis of a biomass post-firing combined-cycle power plant," *Energy*, vol. 77, pp. 553-561, 2014.
[58] M. Al-Soud, E. Hrayshat, "A 50 MW concentrating solar power plant for Jordan," *Journal of Cleaner Production*, vol. 17, no. 6, pp. 625-635, 2009.
[59] J. Choi, J. Ahn, T. Kim, "Performance of a triple power generation cycle combining gas/steam turbine combined cycle and solid oxide fuel cell and the influence of carbon capture," *Applied Thermal Energy*, vol. 71, no. 1, pp. 301-309, 2014.

[60] J. Spelling, B. Laumert, “Thermo-Economic Evaluation of Solar Thermal and Photovoltaic Hybridization Options for Combined-Cycle Power Plants,” *Journal of Engineering for Gas Turbines and Power*, vol 137, no. 3, pp. 311-322, 2015.

[61] S. Gunasekaran, N.D. Mancini, R. El-Khaja, E.J. Sheu, A. Mitsos, “Solar-thermal hybridization of advanced zero emissions power cycle,” *Energy*, vol. 65, pp. 152-165, 2014.

[62] J. Peterseim, U. Hellwig, A. Tadros, S. While, “Hybridisation optimization of concentrating solar thermal and biomass power generation facilities,” *Solar Energy*, vol. 99, pp. 203-214, 2014.

[63] P. Bombarda, C. Invernizzi and M. Gaia, “Performance analysis of OTEC plants with multilevel organic Rankine cycle and solar hybridization,” *Journal of engineering for gas turbines and power*, vol. 135, no. 4, Page 402-410, 2013.

[64] J. Antonanzas, M. Alia-Martinez, F.J. Martinez-de-Pison and F. Antonanzas-Torres, “Towards the hybridization of gas-fired power plants: A case study of Algeria,” *Renewable and Sustainable Energy Reviews*, vol. 51, pp. 116-124, 2015.

[65] D. Popov, “Innovative solar augmentation of gas turbine combined cycle plants”, *Applied Thermal Engineering*, vol. 64, no.1-2, March, pp. 40-50, 2014

[66] H. Ghasemi, E. Sheu, A. Tizzanini, M. Paci and A. Mitsos, “Hybrid solar-geothermal power generation: Optimal retrofitting,” *Applied Energy*, vol.131, pp. 158-170, 2014.

[67] J. Peterseim, S. White, A. Tadros, U. Hellwig, “Concentrated solar power hybrid plants, which technologies are best suited for hybridization?,” *Renewable Energy*, vol. 57, pp. 520-532, 2013.

[68] B. Corona, G. San Miguel and E. Cerrajero, “Life cycle assessment of concentrated solar power (CSP) and the influence of hybridizing with natural gas,” *The International Journal of Life Cycle Assessment*, vol. 19, no. 6, Page 1264-1275, 2014.

[69] J. Hoffmann, G. Vaitilingom, J. Henry, M. Chirtoc, R. Olives, V. Goetz and X. Py, "Temperature dependence of thermophysical and rheological properties of seven vegetable oils in view of their use as heat transfer fluids in concentrated solar plants,” *Solar Energy Materials and Solar Cells*, vol. 178, pp. 129-138, 2018.

[70] A. Yasinskiy, J. Navas, T. Aguilar, R. Alcántara, J. Gallardo, A. Sánchez-Coronilla, E. Martín, D. De Los Santos and C. Fernández-Lorenzo, "Dramatically enhanced thermal properties for TiO 2 -based nanofluids for being used as heat transfer fluids in concentrating solar power plants,” *Renewable Energy*, vol. 119, pp. 809-819, 2018.

[71] Y. Yüksel, "Thermodynamic assessment of modified Organic Rankine Cycle integrated with parabolic trough collector for hydrogen production,” *International Journal of Hydrogen Energy*, vol. 43, no. 11, pp. 5832-5841, 2018.

[72] E. Bellos and C. Tzivanidis, "Investigation of a hybrid ORC driven by waste heat and solar energy,” *Energy Conversion and Management*, vol. 156, pp. 427-439, 2018.

[73] M. Reis and W. Gallo, "Study of waste heat recovery potential and optimization of the power production by an organic Rankine cycle in an FPSO unit," *Energy Conversion and Management*, vol. 157, pp. 409-422, 2018.
[74] J. Sarkar, "Generalized pinch point design method of subcritical-supercritical organic Rankine cycle for maximum heat recovery," *Energy*, vol. 143, pp. 141-150, 2018.
[75] S. Katulić, M. Čehil and D. Schneider, "Exergoeconomic optimization of a combined cycle power plant's bottoming cycle using organic working fluids", *Energy Conversion and Management*, vol. 171, pp. 1721-1736, 2018.
[76] D. Cocco, M. Petrollese and V. Tola, "Exergy analysis of concentrating solar systems for heat and power production", Energy, vol. 130, pp. 192-203, 2017.
[77] S. Toghyani, E. Baniasadi and E. Afshari, "Thermodynamic analysis and optimization of an integrated Rankine power cycle and nano-fluid based parabolic trough solar collector", *Energy Conversion and Management*, vol. 121, pp. 93-104, 2016.
[78] B. Sivapalan, M. Neelesh Chandran, S. Manikandan, M. Saranprabhu, S. Pavithra and K. Rajan, "Paraffin wax–water nanoemulsion: A superior thermal energy storage medium providing higher rate of thermal energy storage per unit heat exchanger volume than water and paraffin wax," *Energy Conversion and Management*, vol. 162, pp. 109-117, 2018.
[79] Y. Fang, J. Niu and S. Deng, "Numerical analysis for maximizing effective energy storage capacity of thermal energy storage systems by enhancing heat transfer in PCM," *Energy and Buildings*, vol. 160, pp. 10-18, 2018.
[80] G. Alva, Y. Lin and G. Fang, "An overview of thermal energy storage systems," *Energy*, vol. 144, pp. 341-378, 2018.
[81] P. Ward, J. Teprovich, Y. Liu, J. He and R. Zidan, "High temperature thermal energy storagein the CaAl 2 system," *Journal of Alloys and Compounds*, vol. 735, pp. 2611-2615, 2018.
[82] B. Nandi, S. Bandyopadhyay and R. Banerjee, "Numerical modeling and analysis of dual medium thermocline thermal energy storage," *Journal of Energy Storage*, vol. 16, pp. 218-230, 2018.
[83] S. Nyamsi, M. Lototskyy and I. Tolj, "Selection of metal hydrides-based thermal energy storage: Energy storage efficiency and density targets," International Journal of Hydrogen Energy, 2018.
[84] R. Lugolole, A. Mawire, K. Lentswe, D. Okello and K. Nyeinga, "Thermal performance comparison of three sensible heat thermal energy storage systems during charging cycles," *Sustainable Energy Technologies and Assessments*, vol. 30, pp. 37-51, 2018.
[85] A. Mehrabadi and M. Farid, "New salt hydrate composite for low-grade thermal energy storage," *Energy*, vol. 164, pp. 194-203, 2018.
[86] G. Peiró, J. Gasia, L. Miró, C. Prieto and L. Cabeza, "Influence of the heat transfer fluid in a CSP plant molten salts charging process," *Renewable Energy*, vol. 113, pp. 148-158, 2017.
[87] B. Bozkaya and W. Zeiler, "The effectiveness of night ventilation for the thermal balance of an aquifer thermal energy storage," *Applied Thermal Engineering*, vol. 146, pp. 190-202, 2018.
[88] M. Schaefer and A. Thess, "Simulation of a closed low-pressure honeycomb adsorber for thermal energy storage," *International Journal of Heat and Mass Transfer*, vol. 126, pp. 796-807, 2018.

[89] T. Başer and J. McCartney, "Transient evaluation of a soil-borehole thermal energy storage system," *Renewable Energy*, 2018.
[90] K. Xie, Y. Nian and W. Cheng, "Analysis and optimization of underground thermal energy storage using depleted oil wells," *Energy*, vol. 163, pp. 1006-1016, 2018.
[91] P. Ward, J. Teprovich, Y. Liu, J. He and R. Zidan, "High temperature thermal energy storage in the CaAl2 system," *Journal of Alloys and Compounds*, vol. 735, pp. 2611-2615, 2018.
[92] W. Sun, X. Yue and Y. Wang, "Exergy efficiency analysis of ORC (Organic Rankine Cycle) and ORC-based combined cycles driven by low-temperature waste heat," *Energy Conversion and Management*, vol. 135, pp. 63-73, 2017.
[93] S. Kalogirou, "A detailed thermal model of a parabolic trough collector receiver," *Energy*, vol. 48, no. 1, pp. 298-306, 2012.
[94] W. Short, D. Packey and T. Holt, *A Manual for the Economic Evaluation of Energy Efficiency and Renewable Energy Technologies*, 1995.
[95] "How much carbon dioxide is produced when different fuels are burned? - FAQ - U.S. Energy Information Administration (EIA)" Internet: https://www.eia.gov/tools/faqs/faq.php?id=73andt=11, Dec. 28, 2014 [Jun. 18 2018].
[96] "Dubai Electricity and amp; Water Authority | tariff", Internet: https://www.dewa.gov.ae/en/customer/services/consumption-services/tariff. May. 08, 2018 [Jun. 29, 2018].

Vita

Mohammed Fouad Azfar Khan was born in 1991 in Dubai, United Arab Emirates. He started his education from Dubai Scholars Private School where he completed his Ordinary Levels in 2007 and completed his Advanced Levels in 2009 from St. Mary's Catholic High School, Dubai. He then joined the American University of Sharjah with Merit Scholarship to start his undergraduate studies in Mechanical Engineering. He graduated with a BSc. in Mechanical Engineering in May 2013.

Mr. Mohammed Fouad began his graduate studies at the American University of Sharjah, for a Master's of Science in Mechanical Engineering, where he received the graduate studies assistantship award. During his M.Sc., Mr. Mohammed Fouad worked as a lab assistant till 2016 in the Department of Mechanical Engineering. Since November 2016, he started working as a Site Engineer for a MEP contracting firm.